2010

Modeling the locked-wheel skid tester to determine the effect of pavement roughness on the International Friction Index

Patrick Cummings
University of South Florida

Modeling the Locked-Wheel Skid Tester to Determine the Effect of Pavement Roughness on the International Friction Index

by

Patrick Cummings

A thesis submitted in partial fulfillment
of the requirements for the degree of
Master of Science in Civil Engineering
Department of Civil and Environmental Engineering
College of Engineering
University of South Florida

Major Professor: Manjriker Gunaratne, Ph.D.
Abdul Pinjari, Ph.D.
Qing Lu, Ph.D.

Date of Approval:
June 11, 2010

Keywords: speed constant, dynamic load coefficient, measured skid number, friction prediction, megatexure

DEDICATION

I dedicate this manuscript to my wife Heather, without whom I would not have had the courage to finish, and to my parents Russell and Marcie, who instilled in me the thirst for knowledge.

ACKNOWLEDGMENTS

I would like to thank Dr. Manjriker Gunaratne for giving me the opportunity to participate in the Masters Degree program. He inspired and provoked the thoughts related to this manuscript. I would also like to thank Dr. Abdul Pinjari and Dr. Qing Lu for agreeing to serve on my committee. Special thanks to the members of my research group who helped me to complete my research and testing.

TABLE OF CONTENTS

LIST OF TABLES

LIST OF FIGURES

Modeling the Locked-Wheel Skid Tester to Determine the Effect of Pavement Roughness on the International Friction Index

Patrick Cummings

ABSTRACT

Pavement roughness has been found to have an effect on the coefficient of friction measured with the Locked-Wheel Skid Tester (LWT) with measured friction decreasing as the long wave roughness of the pavement increases. However, the current pavement friction standardization model adopted by the American Society for Testing and Materials (ASTM), to compute the International Friction Index (IFI), does not account for this effect. In other words, it had been previously assumed that the IFI's speed constant (S_P), which defines the gradient of the pavement friction versus speed relationship, is an invariant for any pavement with a given mean profile depth (MPD), regardless of its roughness. This study was conducted to quantify the effect of pavement roughness on the IFI's speed constant. The first phase of this study consisted of theoretical modeling of the LWT using a two-degree of freedom vibration system. The model parameters were calibrated to match the measured natural frequencies of the LWT. The calibrated model was able to predict the normal load variation during actual LWT tests to a reasonable accuracy. Furthermore, by assuming a previously developed skid number (SN) versus normal load relationship, even the friction profile of the LWT during an actual test was predicted reasonably accurately. Because the skid number (SN) versus normal load

relationship had been developed previously using rigorous protocol, a new method that is more practical and convenient was prescribed in this work. This study concluded that higher pavement long-wave roughness decreases the value of the $\boldsymbol{S_P}$ compared to a pavement with identical MPD but lower roughness. Finally, the magnitude of the loss of friction was found to be governed by the non-linear skid number versus normal load characteristics of a pavement.

CHAPTER 1

INTRODUCTION

1.1 Background

Evaluation and maintenance of friction in all pavement sections of a highway network is a crucial task of transportation safety programs. The frictional interaction between vehicle tires and pavement has been studied at many levels, and significant efforts have been made to determine the factors that govern its mechanism. In early stages of highway pavement maintenance, pavement friction was measured and quantified using static testing devices combined with theoretical physical models. At that time, the principal attributes of friction were assumed to be centered solely on pavement texture. As technology improved, full-scale dynamic friction testing devices that resembled the vehicles in motion in terms of the magnitude of pavement friction experienced, were developed.

It has been found recently that pavement friction is, in fact, governed by several factors including pavement lubrication, pavement roughness, and vehicle behavior in addition to pavement texture. Innovative friction measuring devices are constantly being developed with the measuring mechanisms of each being different from the others. However, most of the current devices in use have been found to produce significantly different results when used on the same pavement [2]. This observation has led to

research regarding harmonization of devices and standardization of the friction evaluations.

1.2 Principles of Pavement Friction

The coefficient of pavement friction, $\boldsymbol{\mu}$, is defined as follows:

$$\mu = \frac{F}{W} \tag{1a}$$

where $\boldsymbol{F}$ is the friction force exerted by the pavement on a wheel and $\boldsymbol{W}$ is the normal load of the device acting on that pavement. However, full-scale friction testing devices quantify and report pavement friction as the Skid Number, $\boldsymbol{SN}$, defined as;

$$SN = 100 * \mu \tag{1b}$$

It has been shown that the slip speed, $\boldsymbol{S}$, at which friction is measured, has a significant effect on the value of the measured $\boldsymbol{SN}$.

$$S = V_V * \%Slip \tag{1c}$$

where $\boldsymbol{V_V}$ is the vehicle speed and the Percent Slip is determined by Equation 1d.

$$\%Slip = \frac{V_V - V_T}{V_V} \tag{1d}$$

$\boldsymbol{V_T}$ is the speed of rotation of the tire during the test. The Penn State Model [1] expresses the speed dependency of $\boldsymbol{SN}$ as follows;

$$SN_S = SN_0 e^{-\frac{PNG}{100}S} \tag{2}$$

where $\boldsymbol{SN_S}$ is the skid number measured at a slip speed of $\boldsymbol{S}$, $\boldsymbol{SN_0}$ is the skid number at zero speed, and $\boldsymbol{PNG}$ is the percent normalized gradient expressing the rate of decrease of friction with speed. $\boldsymbol{SN_0}$ is a factor that has been highly correlated to the pavement microtexture, and $\boldsymbol{PNG}$ is presumed to be dependent only on the pavement macrotexture.

SN_0 and PNG can be determined from linear regression of friction data at various speeds using Equation 2.

In order to address the need for standardization of measurement of different devices, the Permanent International Association of Road Congresses (PIARC) [2] met in France in 1995 to coordinate and conduct an experiment to standardize full-scale pavement friction testing. This experiment, known as the *International PIARC Experiment to Compare and Harmonize Texture and Skid Resistance Measurements*, encompassed sixty-seven parameters from fifty-four pavement sites measured by forty-seven different devices from sixteen countries [2]. Based on the analysis of the results, the International Friction Index (IFI) concept was developed. Subsequently, the American Society for Testing and Materials (ASTM) adopted the IFI and formulated the *Standard Practice for Calculating International Friction Index of a Pavement Surface (E1960-07-2009)* [3].

The IFI standard is a calibration method in which full-scale friction testers are calibrated against a static friction tester, the Dynamic Friction Tester (DFT). The DFT measured friction value at 20 km/h, DFT_{20}, is used as a baseline for calibration. In order to express the speed dependency of friction, the following PIARC model has been developed by revising the Penn State Model [2];

$$FR_S = FR_0 e^{-\frac{S}{S_P}} \tag{3}$$

where FR_S is friction measure at a slip speed S, FR_0 is the friction at zero speed, and S_P is the speed gradient which expresses the rate at which friction reduces with speed. Just as in the case of the original Penn State Model [2] in Equation 2, FR_0 has been highly correlated to pavement microtexture, while S_P has been shown to be correlated to a

pavement's mean profile depth (MPD). The CT Meter is the standard laser device that is recommended for evaluation of the macrotexture of a pavement in terms of MPD. $\boldsymbol{FR_0}$ and $\boldsymbol{S_P}$ can be found using linear regression of friction data acquired at varying speeds, using Equation 3.

In order to calibrate full-scale friction measuring devices using Equation 3, the $\boldsymbol{FR_{60}}$ values of a given pavement measured with a full-scale device are compared to the $\boldsymbol{F_{60}}$ values gathered by the DFT on the same pavement [2]. The $\boldsymbol{FR_{60}}$ values are found by converting friction values found at various speeds back to the friction value at 60 km/h using the $\boldsymbol{S_P}$ value of the pavement measured with the CT meter using the rearranged form of Equation 4;

$$FR_{60}=FR_S e^{-\frac{S-60}{S_P}} \tag{4}$$

Then, using linear regression of the corresponding values of $\boldsymbol{FR_{60}}$ and $\boldsymbol{F_{60}}$ for several test sections, the following calibration equation can be developed and subsequently applied to standardize pavement friction measurements at any speed;

$$F_{60}=A+B*FR_{60} \tag{5}$$

where $\boldsymbol{A}$ and $\boldsymbol{B}$ device specific constants. Finally, using $\boldsymbol{F_{60}}$ from Equation 5 and the $\boldsymbol{S_P}$ readings obtained from the CT Meter, the International Friction Index (IFI) of a pavement is reported as $\boldsymbol{[F_{60}, S_P]}$ [2].

1.3 Locked-Wheel Skid Tester

Among the many different types of full-scale friction measuring devices, the Locked-Wheel Skid Tester (LWT) has been known to collect the repeatable and consistent data. It is for this reason that State Departments of Transportation (DOT) and

the Federal Highway Administration (FHWA) have adopted the LWT as the standard friction measuring device. The LWT is a full slip device, since the measurements are carried out at a slip of 100 percent with the measuring wheel completely locked during testing. ASTM regulates the manufacturing and measuring standard of the LWT in *Standard Test Method for Skid Resistance of Paved Surfaces Using a Full-Scale Tire (E274-06-2009)* [4].

1.4 Limitations of the International Friction Index

The above IFI concept has inherent limitations because the dynamic effects experienced by full-scale testing devices such as the LWT are not fully expressed when calibrated against a static testing device such as the DFT. It has been documented that pavement long-wave roughness has a significant effect on the measured skid values [5]. Pavement long-wave roughness, also known as the megatexture, causes the normal load of the measuring device to fluctuate. This normal load fluctuation can be quantified by the Dynamic Load Coefficient, ***DLC***, expressed as;

$$DLC = \frac{\sigma_W}{W_{STATIC}} \tag{6a}$$

where $\boldsymbol{\sigma_W}$ is the standard deviation of the normal load and $\boldsymbol{W_{STATIC}}$ is the static weight of the device. An increased ***DLC*** over a pavement section has been shown to lower the skid values measured by the LWT [5]. This effect is seen to affect the calibrated IFI values of pavements that produce significantly high ***DLC*** values.

The factor contributing to the variation of the measured skid resistance with the ***DLC*** is the dependency of the measured skid values on the normal load. Fuentes et al. [5]

showed that the following approximate equation can be used to express the relationship between normal load and ***SN***;

$$SN = SN_i + \frac{SN_i - SN_r}{1 + e^{-\frac{(W - w_i)}{b}}} \quad (6b)$$

where $\boldsymbol{SN_i}$ is the ***SN*** at relatively low normal loads, $\boldsymbol{SN_r}$ is the ***SN*** at relatively high normal loads, $\boldsymbol{W}$ is the instantaneous normal load, and $\boldsymbol{w_i}$ and $\boldsymbol{b}$ are parameters specific to the LWT. Fuentes' pavement friction dependency on normal load deviations can be compared to the empirical equation developed by Schallamach [6] to express the dependence of rubber friction on the normal load;

$$\mu = cW^{-\frac{1}{3}} \quad (7)$$

where $\boldsymbol{\mu}$ is the observed friction, $\boldsymbol{W}$ is the normal load, and $\boldsymbol{c}$ is dependent on the velocity.

1.5 Objectives of Study

Due to the above discussed limitations of the IFI and the observed effect of ***DLC*** on measured skid values, an investigation was proposed to further quantify the effects of ***DLC*** on the IFI. By theoretically modeling the dynamics of the LWT and comparing the model's predicted behavior with the corresponding field measurements, the effect of pavement roughness on the IFI calibration standard would be quantified.

CHAPTER 2

EXPERIMENTAL ANALYSIS AND RESULTS

2.1 Proposed Vibration Modeling System

In previous research completed at the University of South Florida (USF) [5], it was shown that the dominant natural frequency of the LWT is approximately 1.9 Hz. An additional natural frequency around 11 Hz was also revealed, but with a nearly damped out corresponding deflection. Therefore, a damped two-degree of freedom system with a dominant natural frequency close to 1.9 Hz is proposed to model the LWT appropriately. Figure 2.1 illustrates the proposed model and the associated parameters;

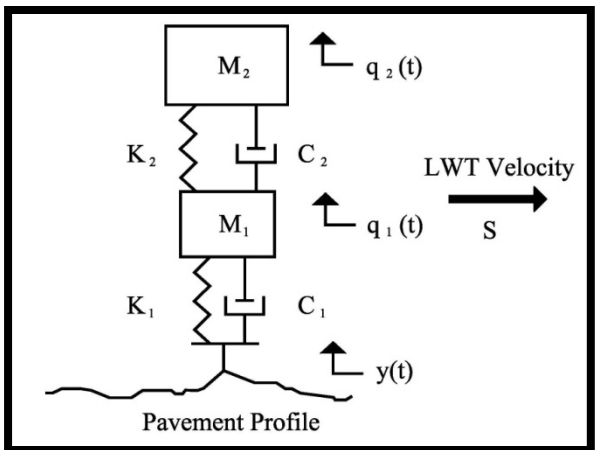

Figure 2-1: Two Degree of Freedom System with Displacement Input

M_1 is the mass of the first degree of freedom of the model, and its displacement is given by the function $q_1(t)$. K_1 and C_1 are the respective spring constant and damping value for the first degree of freedom of the model. M_2 is the mass of the second degree of freedom

of the model, and its displacement is given by the function $q_2(t)$. K_2 and C_2 are the respective spring constant and damping value for the second degree of freedom of the model. The input for the proposed model is a displacement corresponding to the pavement profile, $y=f(x)$, that is transformed into a time dependent vertical displacement input, $y=f(t)$, using the following equation;

$$t=\frac{x}{S} \tag{8}$$

where x is the longitudinal distance along the pavement profile, and S is the speed of the LWT. The proposed modeling program was built around the following equation of motion in space state form;

$$\dot{z}=A\underline{z}+\underline{B}y+\underline{C}\dot{y} \tag{9}$$

where $\underline{z}$ is the array of state of variables in Equation 10, A, $\underline{B}$, and $\underline{C}$, are array variables in Equations 11, 12, and 13, $\dot{y}$ is the first derivative of the pavement profile with respect to time, and $\dot{z}$ is the first derivative of the variable z.

$$\underline{z}=[q_2 \;\; \dot{q}_2 \;\; q_1 \;\; \dot{q}_1] \tag{10}$$

$$A=\begin{bmatrix} 0 & 1 & 0 & 0 \\ -\frac{K_2}{M_2} & -\frac{C_2}{M_2} & \frac{K_2}{M_2} & \frac{C_2}{M_2} \\ 0 & 0 & 0 & 1 \\ \frac{K_2}{M_1} & \frac{C_2}{M_1} & -\frac{(K_2+K_1)}{M_1} & -\frac{(C_2+C_1)}{M_1} \end{bmatrix} \tag{11}$$

$$\underline{B}=\begin{bmatrix} 0 & 0 & 0 & \frac{K_1}{M_1} \end{bmatrix}^T \tag{12}$$

$$\underline{C}=\begin{bmatrix} 0 & 0 & 0 & \frac{C_1}{M_1} \end{bmatrix}^T \tag{13}$$

Using the above variables, the following numerical forms of the first and second derivatives of the displacement functions, $q_1(t)$ and $q_2(t)$, were used to solve for the system's response explicitly;

$$\dot{q}_i(t) = \frac{q_i(t+\Delta t) - q_i(t-\Delta t)}{2\Delta t} \tag{14}$$

$$\ddot{q}_i(t) = \frac{q_i(t+\Delta t) + q_i(t-\Delta t) - 2q_i(t)}{\Delta t^2} \tag{15}$$

A Microsoft Excel program, *LWT Prediction Model*, was developed to solve Equations 8-15 and hence model the response of two degree of freedom systems.

2.2 Verification of the Program

Due to the fact that the developed program has the capacity to model any given two degree of freedom system that experiences a time dependent displacement input, several verifications were conducted to ensure the accuracy of the program. These verifications are outlined in the following sections.

2.2.1 Modeling of a Two Degree of Freedom System Without Damping

Since the vibration response of damped systems is relatively complex, the verifications started with an undamped two degree of freedom system. Das [7] shows that the natural frequencies of an undamped two degree of freedom system can be found using the following closed form solutions:

$$\omega_{1n} = \frac{1}{\sqrt{2}}\left\{\left(\frac{K_1+K_2}{M_1} + \frac{K_2}{M_2}\right) + \left[\left(\frac{K_1+K_2}{M_1} - \frac{K_2}{M_2}\right)^2 + \frac{4K_2^2}{M_1M_2}\right]^{\frac{1}{2}}\right\}^{\frac{1}{2}} \tag{16}$$

$$\omega_{2n} = \frac{1}{\sqrt{2}}\left\{\left(\frac{K_1+K_2}{M_1} + \frac{K_2}{M_2}\right) - \left[\left(\frac{K_1+K_2}{M_1} - \frac{K_2}{M_2}\right)^2 + \frac{4K_2^2}{M_1M_2}\right]^{\frac{1}{2}}\right\}^{\frac{1}{2}} \tag{17}$$

where the parameters are described by the proposed model in Figure 2-1. Table 2-1 shows the parameters for one sample model in which undamped natural frequencies were obtained using the above closed form solutions.

Table 2-1: Model Parameters for a Two Degree of Freedom System Without Damping

$\mathbf{M_2}$	100	Kg
$\mathbf{M_1}$	100	Kg
$\mathbf{C_2}$	0	N*s/m
$\mathbf{C_1}$	0	N*s/m
$\mathbf{K_2}$	10000	N/m
$\mathbf{K_1}$	10000	N/m

The frequency spectrum was generated for the above system using the computer program *LWT Prediction Model*. This is shown in Figure 2-2, which displays the system's two natural frequencies at 16.2 Hz and 6.2 Hz. From the closed-form solutions in Equations 16 and 17, the natural frequencies were found to be 16.180 Hz and 6.180 Hz respectively. Figure 2-2 also shows that the frequency response of the program agrees well with the corresponding closed-form solutions.

2.2.2 Modeling of an Uncoupled Two Degree of Freedom System With Damping

The natural frequencies of some damped two degree of freedom systems can be found by uncoupling the damping parameters from the stiffness parameters and solving the eigenvalue problem. To verify that the response of the developed program was accurate with damping, a solved example from Inman [8] was modeled for verification of the program. Table 2-2 shows the system parameters of the damped vibration system used in this case.

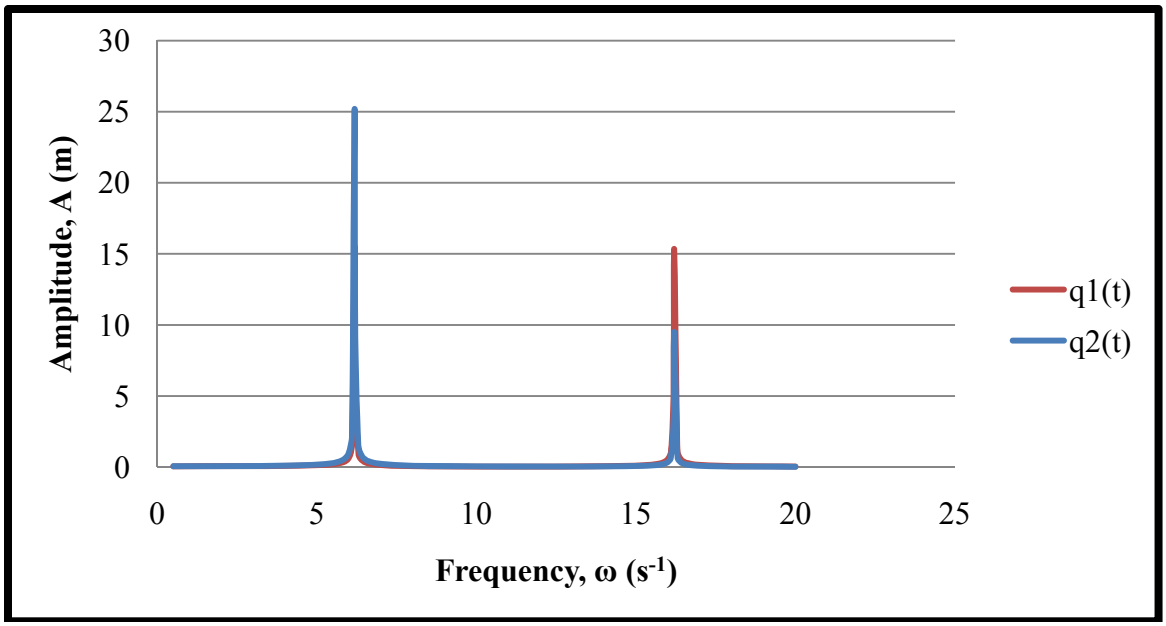

Figure 2-2: Frequency Spectrum of a Two Degree of Freedom System Without Damping

Table 2-2: Model Parameters for a Two Degree of Freedom System With Damping

$\mathbf{M_2}$	1	Kg
$\mathbf{M_1}$	1	Kg
$\mathbf{C_2}$	1	N*s/m
$\mathbf{C_1}$	2	N*s/m
$\mathbf{K_2}$	4	N/m
$\mathbf{K_1}$	5	N/m

According to Inman's solution, the natural frequencies of the first and second degrees of freedom of the system described by Table 2-2 are 3.33 Hz and 1.343 Hz respectively. The above system was then used as an input in the computer program *LWT Prediction Model* and the frequency spectrum was generated to determine the two natural frequencies. Figure 2-3 shows that the program results agree well with the two natural frequencies derived by Inman [8].

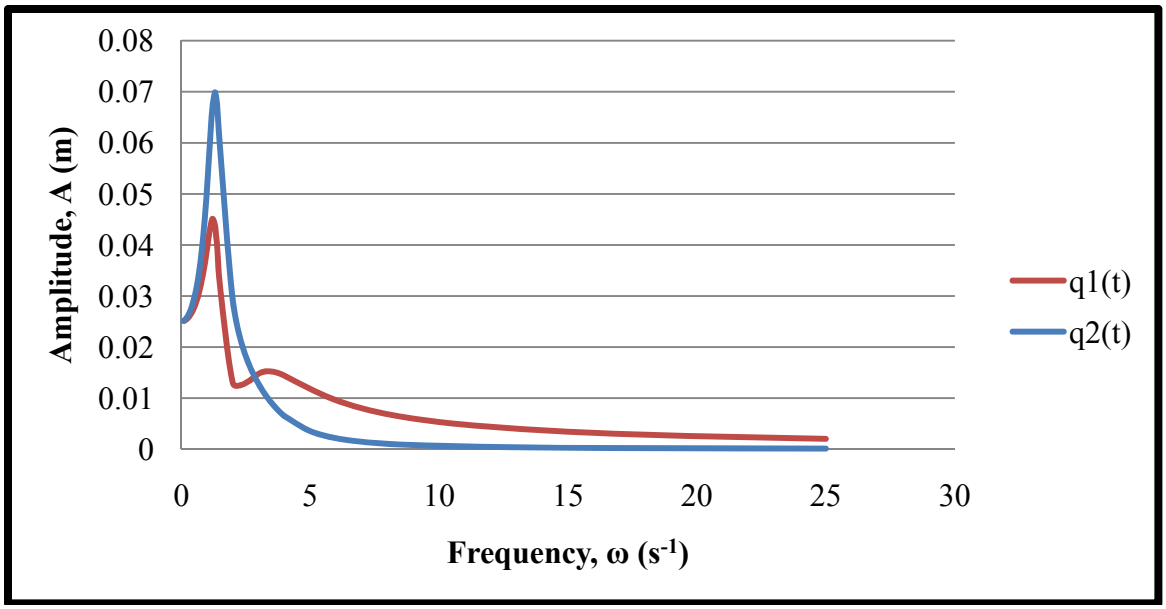

Figure 2-3: Frequency Spectrum of a Two Degree of Freedom System With Damping

2.2.3 Modeling of a One Degree of Freedom System With Damping

Damped one degree of freedom systems can be solved relatively easily for their natural frequencies. Due to this fact, a two degree of freedom system was selected to emulate the response of two one degree of freedom systems by each time restraining one of the degrees of freedom. In the first of these two cases, the degree of freedom of M_2 was restricted using the parameters presented in Table 2-3, and the natural frequency of the first degree was determined using the following basic equations [8];

$$\omega_{in}=\sqrt{\frac{K_i}{M_i}} \tag{18a}$$

$$\zeta_i=\frac{C_i}{2\sqrt{K_i M_i}} \tag{18b}$$

$$\omega_{id}=\omega_{in}\sqrt{1-\zeta_i} \tag{18c}$$

where M_i, K_i, and C_i correspond to the parameters of the model in Figure 2-1, ω_{ni} is the undamped natural frequency of the i^{th} degree of freedom, ζ_i is the damping ratio of the i^{th} degree of freedom, and ω_{di} is the damped natural frequency of the i^{th} degree of freedom.

Table 2-3: Model Parameters for a One Degree of Freedom System Restricting the Motion of M_2

M_2	10	Kg
M_1	1000	Kg
C_2	0	N*s/m
C_1	5000	N*s/m
K_2	20000	N/m
K_1	20000	N/m

According to Equations 18a-18c, the natural frequency of the first degree of the above system is 3.708 Hz. Then, the above parameters were input to the program and a frequency spectrum was generated to determine the system's natural frequency. Figure 2-4 shows that the corresponding natural frequency is 3.7 Hz. Also, one can see that the first and second degrees of freedom coincided, thus verifying the simplified one degree of freedom motion anticipated in this case.

In the second case, M_1 was made to always follow the input displacement function of the pavement profile. This would allow the second degree of freedom to act freely and describe a single degree of freedom motion. This condition was achieved using the parameters outlined in Table 2-4. The corresponding damped natural frequency of the second degree of freedom was found to be 3.708 Hz using Equations 18a-18c. The above system was then modeled using the program *LWT Prediction Model*, and a frequency spectrum was generated to determine the damped natural frequency. Figure 2-5 shows the

frequency response producing a natural frequency of 3.7 Hz thus verifying the accuracy of the computer program.

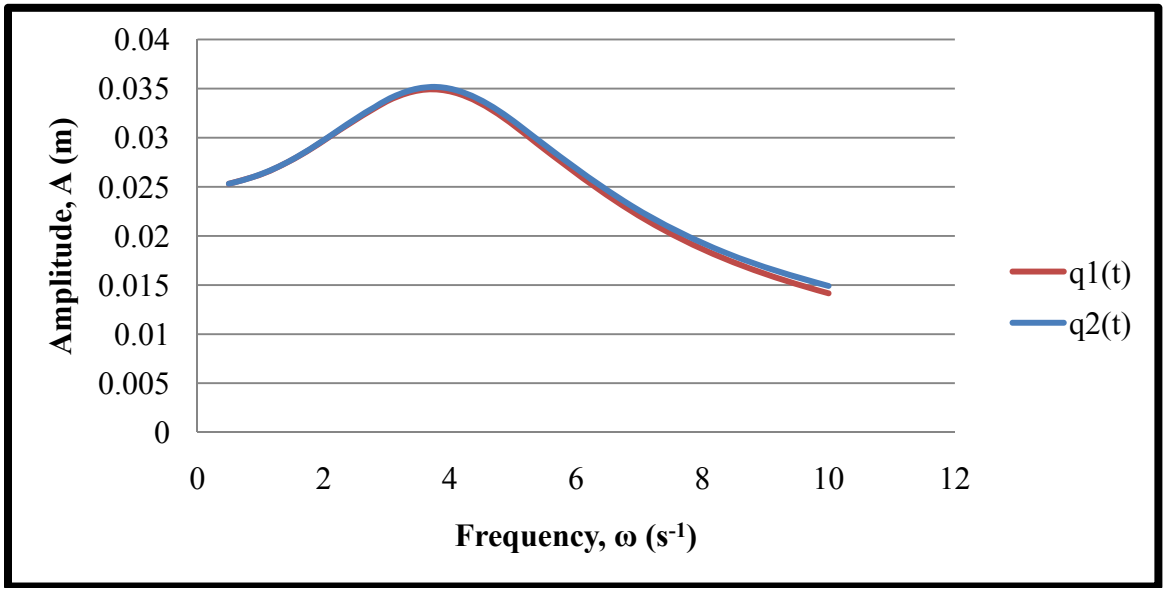

Figure 2-4: Frequency Spectrum of the One Degree of Freedom System Restricting the Motion of M_2

Table 2-4: Model Parameters for a One Degree of Freedom System Restricting the Motion of M_1

M_2	1000	Kg
M_1	-	Kg
C_2	5000	N*s/m
C_1	-	N*s/m
K_2	20000	N/m
K_1	-	N/m

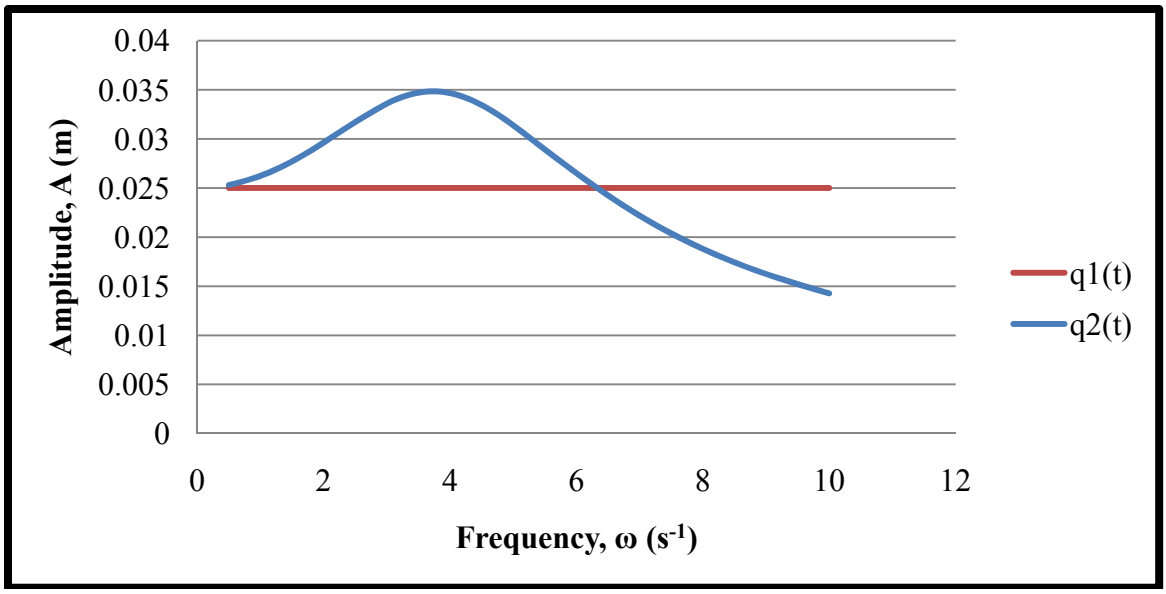

Figure 2-5: Frequency Spectrum of the One Degree of Freedom System Restricting the Motion of M_1

2.3 Determination of LWT Parameters Using Modeling Techniques

After verifying the accuracy of the computer program *LWT Prediction Model*, it was necessary to determine the parameters of a damped two degree of freedom system that closely matched the vertical response of the LWT to any pavement profile. In order to do this, trial combinations of model parameters were iteratively input to the program and the corresponding frequency was determined until the experimentally dominant natural frequency was obtained by the model [5]. As mentioned in Section 2.1, the measured dominant natural frequency of the LWT from previous research [5] was shown to be around 1.9 Hz. Table 2-5 demonstrates the parameters of a system that closely matches the response of the LWT, in terms of the predominant natural frequency.

The frequency response of the modeled two degree of freedom system is represented in Figure 2-6. It is seen that the modeled natural frequency is around 1.9 Hz, which closely matches the experimentally measured dominant natural frequency of 1.9

Hz. The second experimental natural frequency of the LWT was seen to be around 11 Hz, but its amplitude was almost completely damped out. Therefore, the second natural frequency of the above modeled system is insignificant.

Table 2-5: Parameters of a Two Degree of Freedom System Representing the LWT

$\mathbf{M_2}$	440	Kg
$\mathbf{M_1}$	60	Kg
$\mathbf{C_2}$	1000	N*s/m
$\mathbf{C_1}$	250	N*s/m
$\mathbf{K_2}$	5000	N/m
$\mathbf{K_2}$	2000	N/m

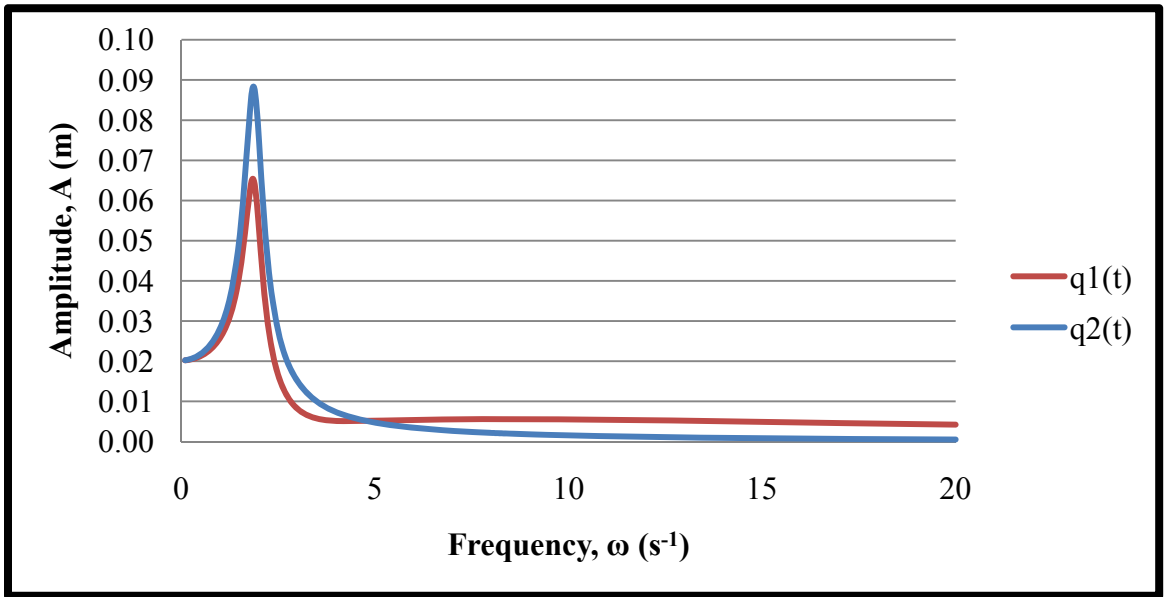

Figure 2-6: Frequency Spectrum of a Two Degree of Freedom System Representing the LWT

2.4 Verification of LWT Parameters Using Field Measurements

In order to model the friction response of the LWT correctly, a comparison was made between the experimental response of the LWT for a given profile to that of the program *LWT Prediction Model* for the same profile. The Profile H tested for this

purpose is shown in Figure 2-7. A series of field tests was conducted at different speeds over the above profile to determine the real time (actual) response of the LWT. This spatial profile was first converted to a time dependent profile for modeling purposes. Finally the profile was input to the computer-based LWT model and normal load response of the modeled LWT was predicted. Figures 2-8, 2-9, and 2-10 show the actual normal load response of the LWT at 20, 40, and 60 mph plotted against the response of the modeled system.

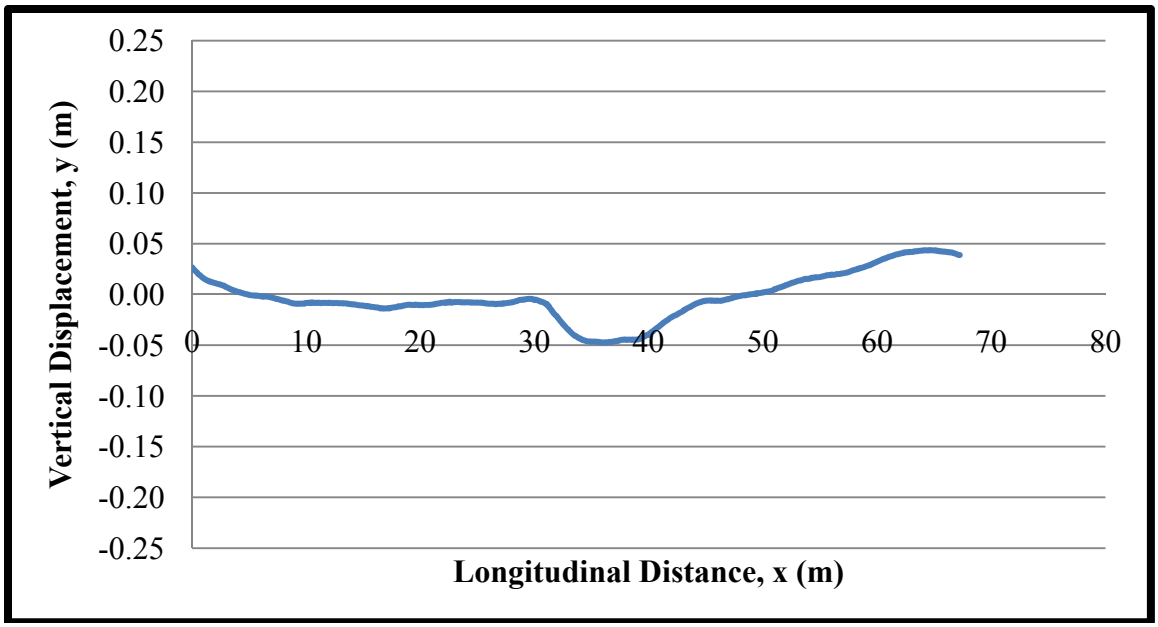

Figure 2-7: Longitudinal Profile of Pavement H

Review of Figures 2-8, 2-9, and 2-10 reveals that the modeled response is more accurate at higher speeds than at lower speeds. This could be attributed to the back torque created by the frictional force which at lower speeds causes the trailer to bounce more vigorously. However, the back torque effects cannot be modeled using the author's simplified system.

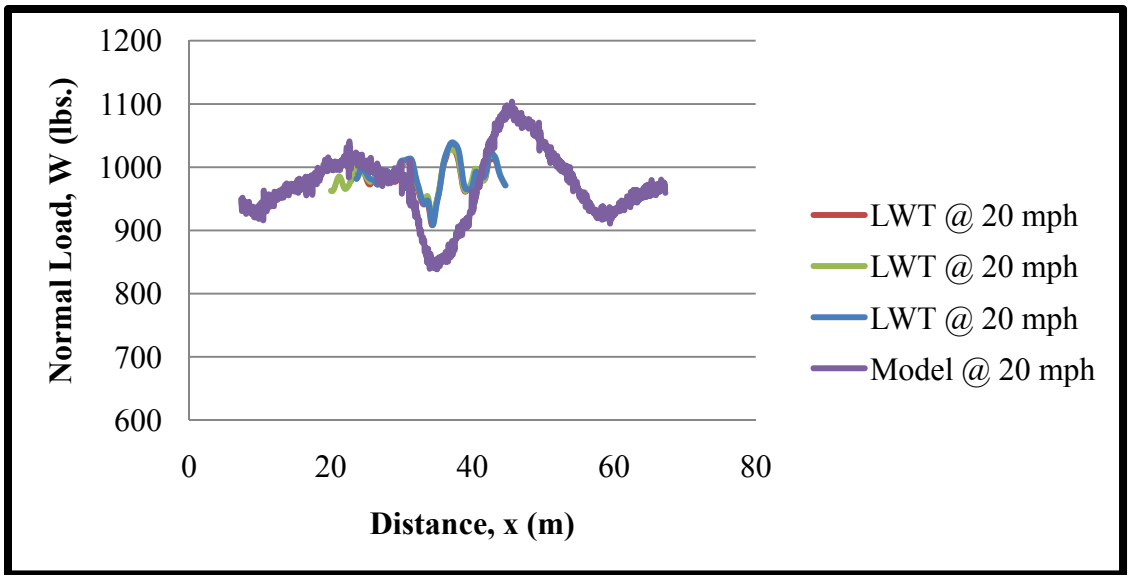

Figure 2-8: Comparison of Experimental and Modeled Response of LWT at 20 mph

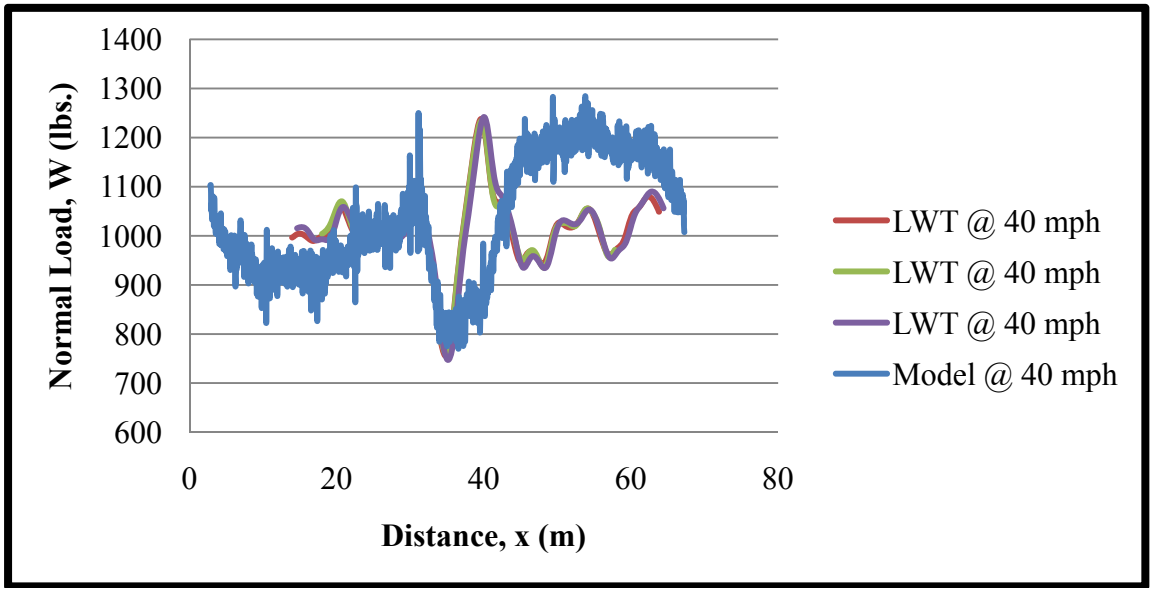

Figure 2-9: Comparison of Experimental and Modeled Response of LWT at 40 mph

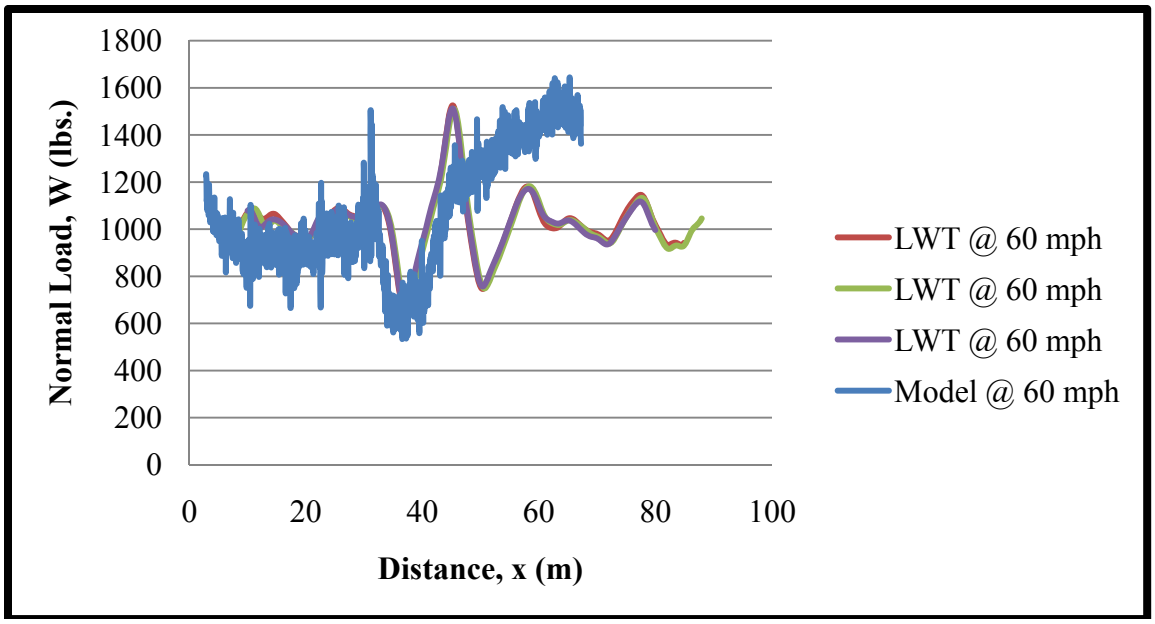

Figure 2-10: Comparison of Experimental and Modeled Response of LWT at 60 mph

Although the overall response of the LWT at 20 mph is not predicted accurately, the predicted average is close to those of the actual response thus showing that the model is somewhat valid even at lower speeds such as 20 mph. On the other hand, at speeds of 40 mph and 60 mph, the deviations in normal load are much more accurate, and prove that the proposed two degree of freedom system represents the response of the LWT more accurately over a given profile at higher speeds.

2.5 Determination of the Relationship Between the Friction and Normal Loads

One objective of this research is to accurately predict the pavement friction measured by an LWT using a two degree of freedom system. After verifying that the normal load deviations are accurately modeled, the next step was to verify the friction predictions of the LWT. In order to predict the frictional force experienced by the LWT on any given pavement, the relationship of friction load to normal load on that pavement

must be determined. In order to perform this task, the relationship between the skid number, ***SN***, and the normal load proposed by Fuentes et al. [5] in equation (6b) will be used. The experimental procedure followed by Fuentes et al. [5] to determine this relationship for a given pavement is rigorous and painstaking. Thus, in order to avoid recreating this experiment, the friction data obtained by Fuentes et al. [5] in the above experiment was used in the author's analysis. Table 2-6 contains the friction data presented by Fuentes et al. [5] for two Pavements C and D. Figures 2-11 and 2-12 illustrate the relationship determined from Equation 6b for speeds of 30 and 55 mph respectively.

The frictional force vs. normal load relationship is deduced by simply multiplying the ***SN*** by the corresponding normal load at any selected point on the curves in Figures 2-11 and 2-12. Figures 2-13 and 2-14 illustrate the corresponding relationships between frictional force and normal load derived from Figures 2-11 and 2-12 respectively.

Table 2-6: Parameters for the ***SN*** vs. ***W*** Relationship for Pavements C and D (Fuentes et al., 2010)

Pavement	**Speed**	**SN_i**	**$\ln(SN_i)$**	**SN_r**	**$\ln(SN_r)$**
C	30	47.5	3.861	41.5	3.726
C	55	42.5	3.750	36.4	3.595
D	30	51.7	3.945	34.5	3.541
D	55	35	3.555	21	3.045

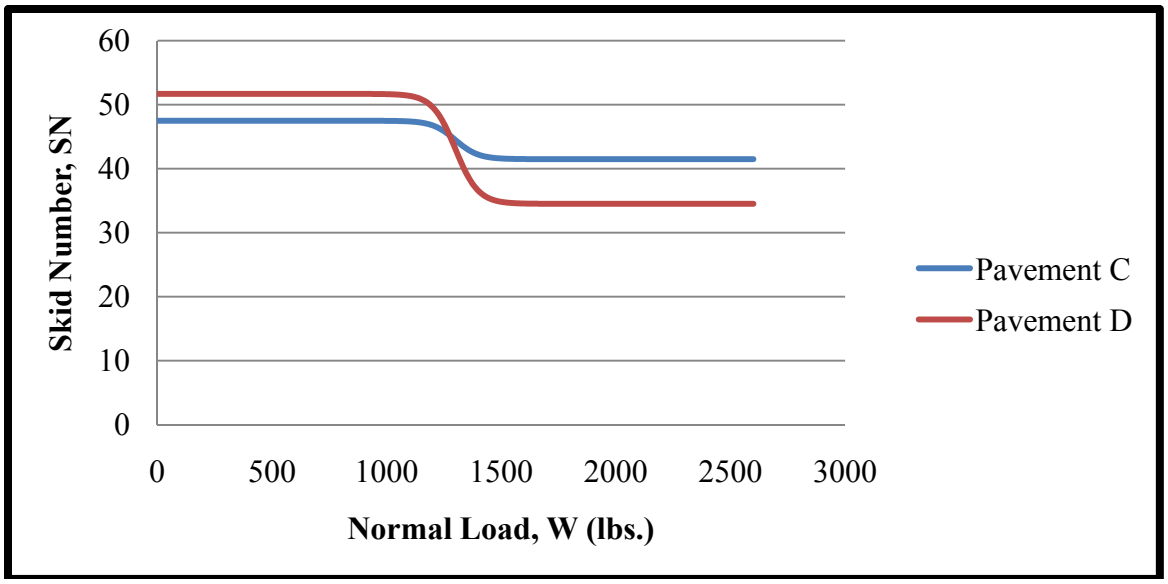

Figure 2-11: ***SN*** vs. ***W*** Relationship at 30 mph (Fuentes et al., 2010)

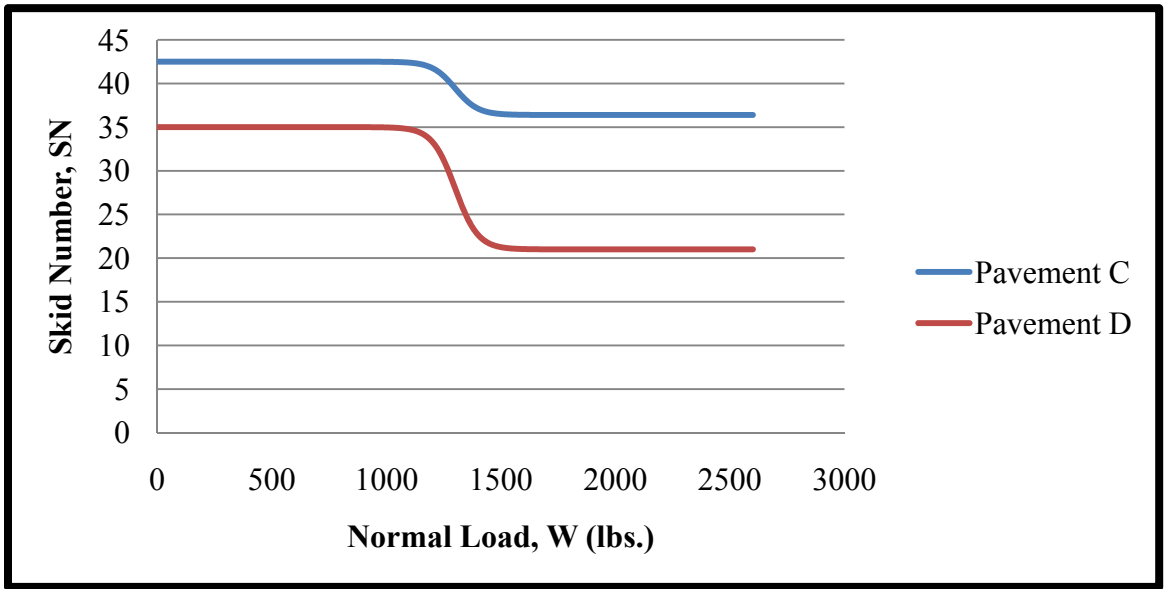

Figure 2-12: ***SN*** vs. ***W*** Relationship at 55 mph (Fuentes et al., 2010)

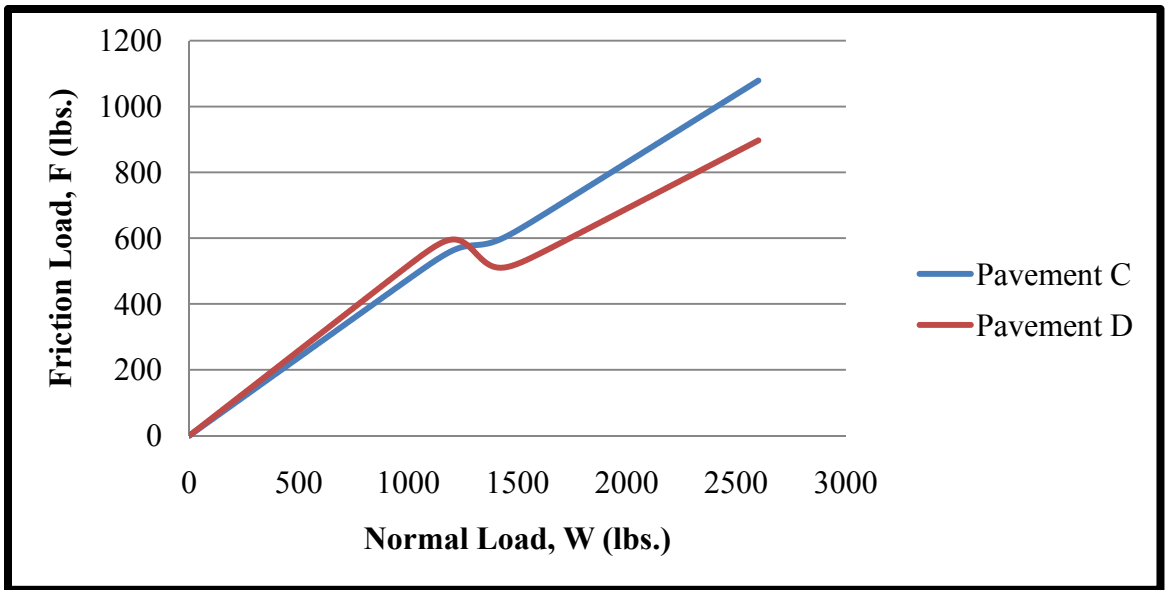

Figure 2-13: Derived Relationship of Frictional Force to Normal Load at 30 mph

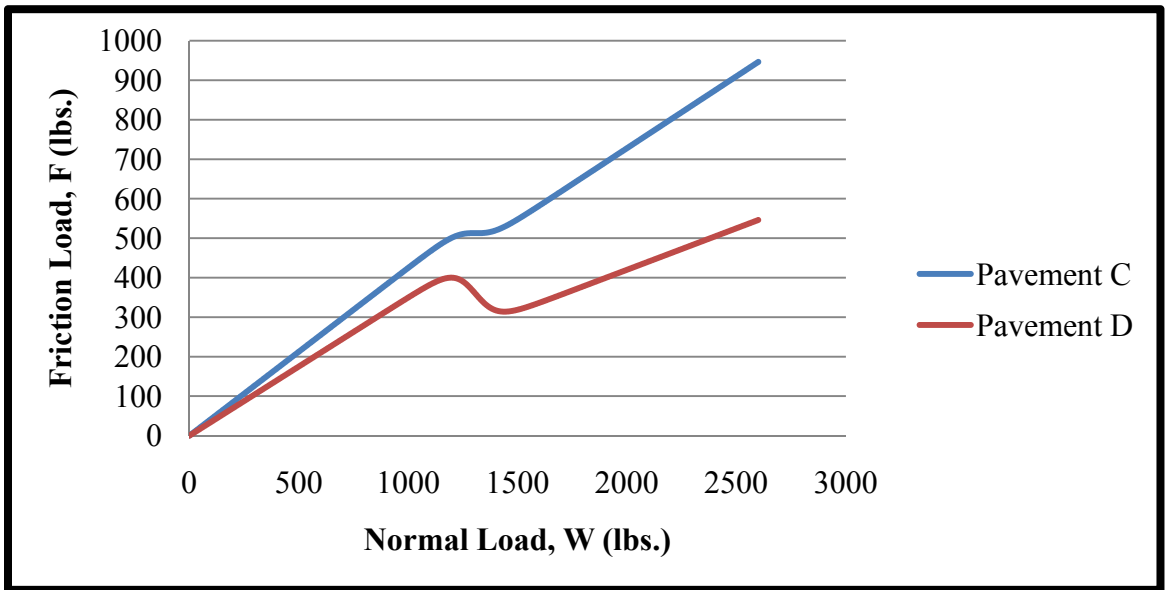

Figure 2-14: Derived Relationship of Frictional Force to Normal Load at 55 mph

In order to model the ***SN*** vs. normal load at speeds other than 30 and 55 mph, a logarithmic re-arrangement of the fundamental friction-speed relationship in Equation 3 can be used as shown in Equation 19.

$$ln(SN) = -\frac{S}{S_P} + ln(SN_0) \quad (19)$$

Figures 2-15 and 2-16 depict how the relationships of SN_i and SN_r versus speed were determined respectively using Equation 19 for Pavement C and D for a range of speeds used in the current analysis.

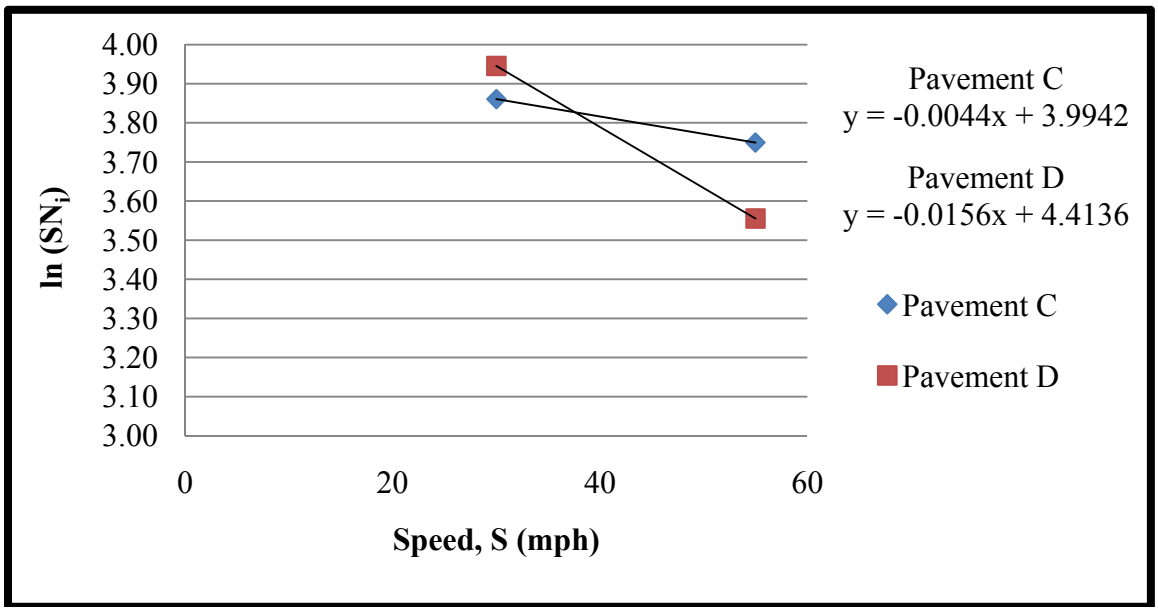

Figure 2-15: Relationship between SN_i and Speed

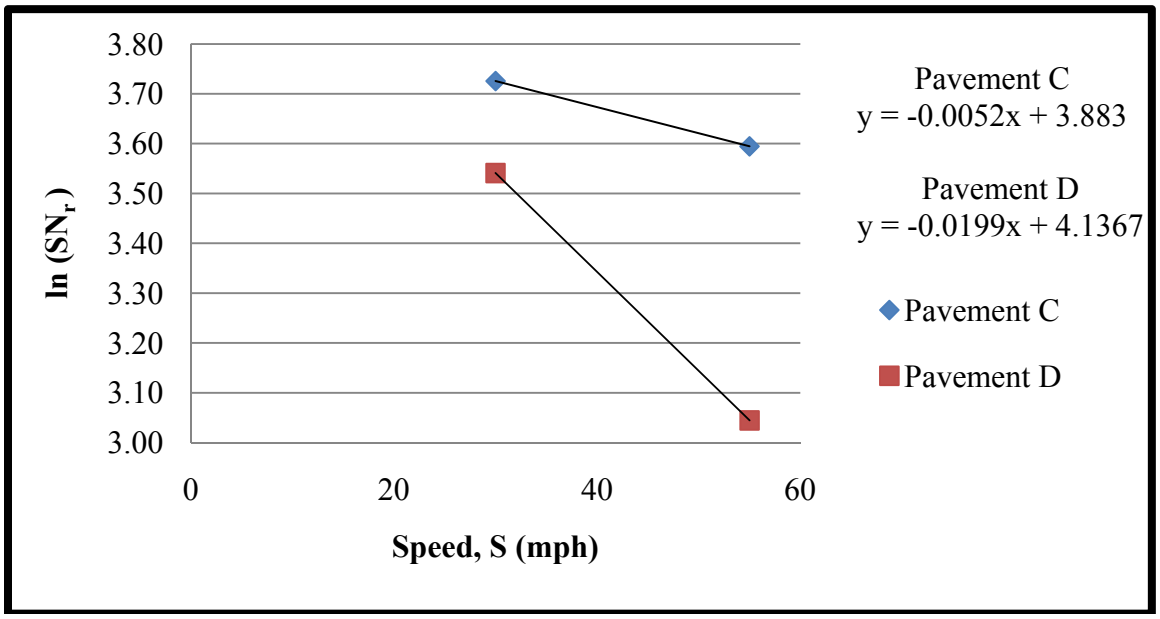

Figure 2-16: Relationship between SN_r and Speed

Tables 2-7 and 2-8 contain data on the variations of SN_i and SN_r with speed generated using Figures 2-15 and 2-16 for Pavements C and D.

Table 2-7: Parameters for Projection of *SN* vs. Normal Load Relationship Across a Range of Speeds for Pavement C (Fuentes et al., 2010)

Pavement	Speed	SN_i	$\ln(SN_i)$	SN_r	$\ln(SN_r)$
C	20	49.710	3.906	43.772	3.779
C	25	48.628	3.884	42.649	3.753
C	30	47.570	3.862	41.554	3.727
C	35	46.535	3.840	40.488	3.701
C	40	45.522	3.818	39.449	3.675
C	45	44.532	3.796	38.436	3.649
C	50	43.563	3.774	37.450	3.623
C	55	42.615	3.752	36.489	3.597
C	60	41.687	3.730	35.552	3.571

Table 2-8: Parameters for Projection of *SN* vs. Normal Load Relationship Across a Range of Speeds for Pavement D (Fuentes et al., 2010)

Pavement	Speed	SN_i	$\ln(SN_i)$	SN_r	$\ln(SN_r)$
D	20	60.437	4.102	42.043	3.739
D	25	55.902	4.024	38.061	3.639
D	30	51.707	3.946	34.457	3.540
D	35	47.827	3.868	31.193	3.440
D	40	44.239	3.790	28.239	3.341
D	45	40.919	3.712	25.564	3.241
D	50	37.849	3.634	23.143	3.142
D	55	35.009	3.556	20.951	3.042
D	60	32.382	3.478	18.967	2.943

Then, the data shown in Tables 2-7 and 2-8 can be used to model the *SN* vs. normal load relationship for Pavements C and D at any speed using Equations 6b and 19.

2.6 Verification of Friction Load Modeling

After determining the relationship of friction load to normal load, an experimental verification was extended to ensure that the program models correctly the friction load experienced by the LWT as well. Using Equation 6b and the data from Tables 2-7 and 2-8 combined with the normal load deviation prediction capability of the modeling program *LWT Prediction Model*, an attempt was made to predict the pavement friction on Pavement H.

Since the experimental procedure to determine the relationships of skid number and friction to normal load were not recreated for Pavement H, it was assumed that the curve corresponding to Pavement H was geometrically similarly to that of Pavement D in Fuentes' experimentation. Therefore, ***SN*** versus normal load (Figure 2-12) and friction load versus normal load (Figure 2-14) curves were replotted in Figures 2-17 and 2-18. In the experiment conducted by Fuentes et al. [5], the $\boldsymbol{SN_0}$ in Equation 6b was found to be the same as the ***SN*** value of the pavement under normal loads used in standard LWT testing conditions. Thus, assuming that the ***SN*** measured at the standard LWT normal load for Pavement H as $\boldsymbol{SN_0}$ corresponding to that pavement, curves for Pavement H in Figures 2-17 and 2-18 were generated for ***SN*** and friction load.

Then, friction tests were conducted on Pavement H using the LWT, and those results were compared to the responses predicted by the modeling program. Figure 2-19 shows the comparison of the model predictions to the actual test results conducted in three trials.

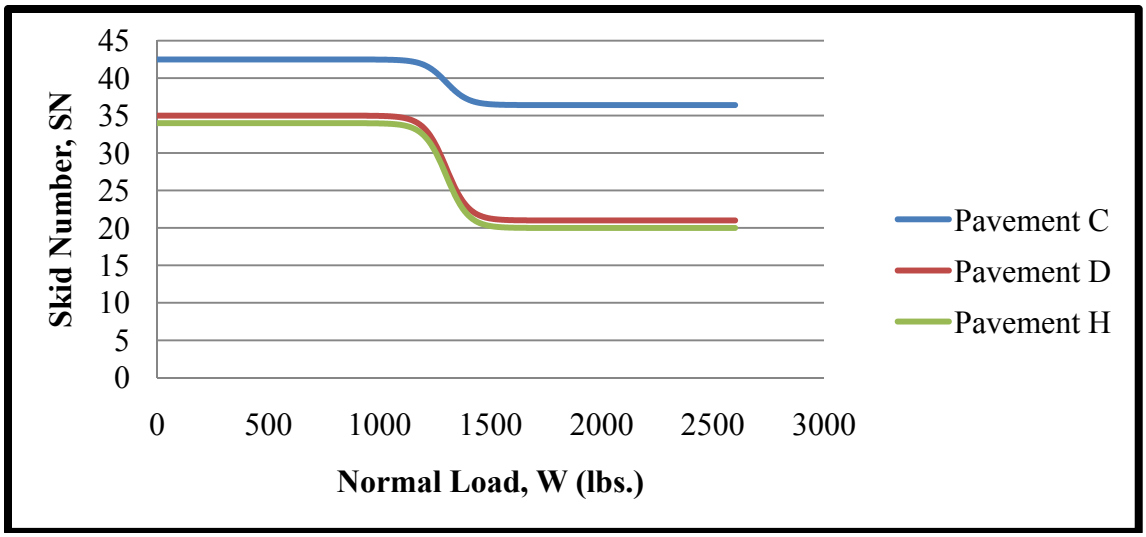

Figure 2-17: Relationship of ***SN*** vs. Normal Load for Pavement H at 55 mph

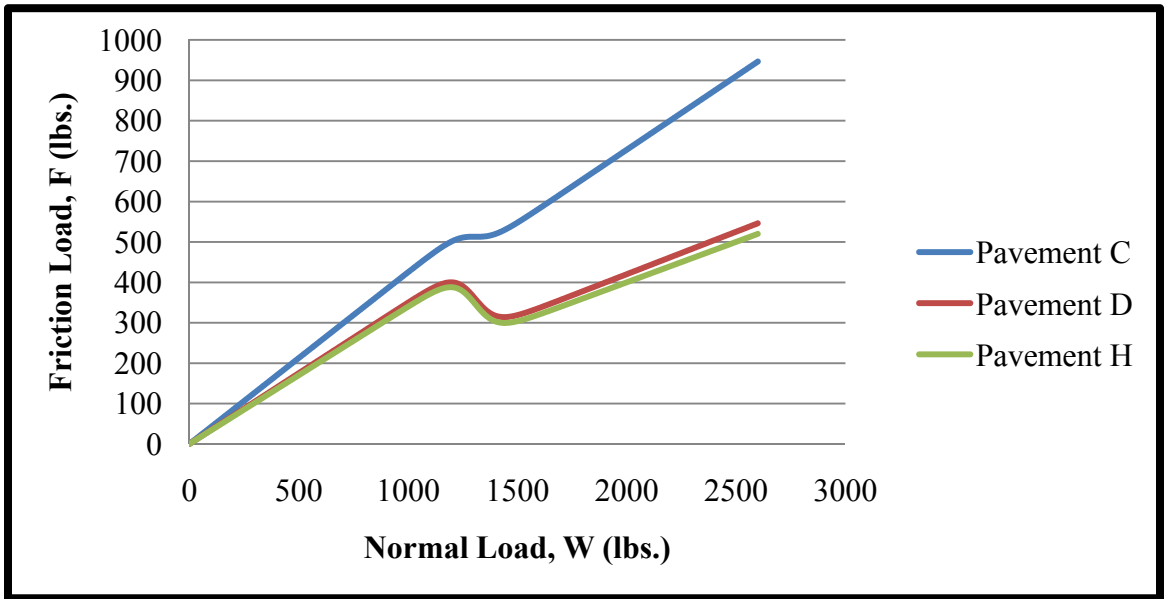

Figure 2-18: Relationship of Friction Load vs. Normal Load for Pavement H at 55 mph

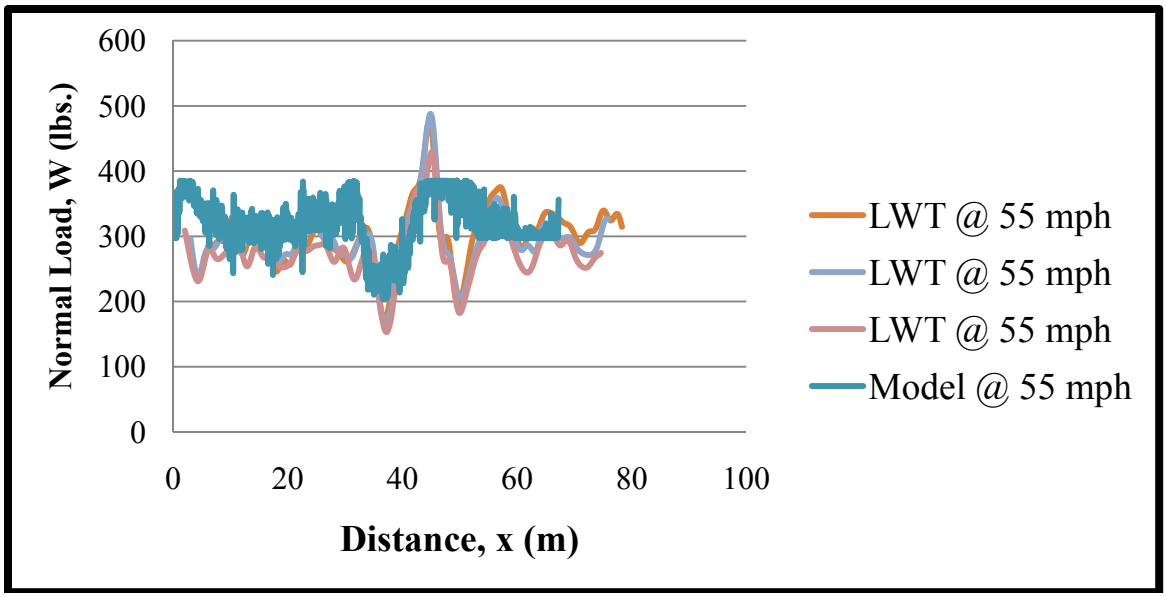

Figure 2-19: Comparison of Model Prediction to the Results of Friction Tests

As one can see from Figure 2-19, the friction load of the pavement is reasonably accurately modeled by the program *LWT Prediction Model*. The average ***SN*** of the skid tests was 29.6, while the program predicted an average of 30.3.

2.7 Modeling the Effects of Pavement Roughness on the IFI

After verifying that the modeling program correctly modeled the normal load and the frictional load deviation of the LWT, friction data from the Fuentes experiment [5] were used to determine the effects of pavement roughness on the IFI parameters. In order to achieve this, an analysis was performed to investigate the individual effects of frequency and amplitude variations on the ***SN*** predicted by the program *LWT Prediction Model*.

First, a range of pavement profiles with varying frequencies with identical amplitudes were modeled by the program *LWT Prediction Model* to determine the effects

of the frequency variations on the friction-speed relationship. Table 2-9 shows the input values of the modeling program.

Table 2-9: Inputs for Frequency Variation Analysis (A = 0.25 m)

Pavement	Frequency, ω (Hz)			
C	0.00	0.05	0.50	5.00
D	0.00	0.05	0.50	5.00

Figures 2-20 and 2-21 display the results corresponding to the above input values.

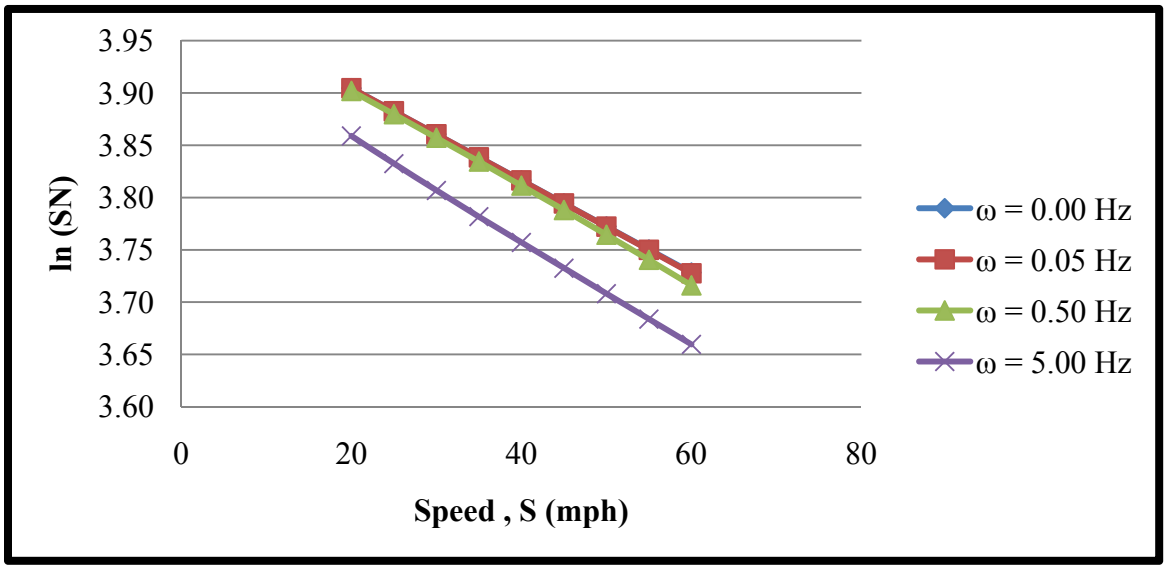

Figure 2-20: Frequency Variation Effects on the Friction-Speed Relationship of Pavement C

The SN_0 evaluated from these plots is the friction value at zero speed. The magnitudes of SN_0 and the changes of the slope of the friction-speed relationship (speed gradient) for Pavements C and D are shown in Table 2-10. As seen in Table 2.10, for a given pavement, as the frequency increases the gradient of the friction versus speed curve

increases while the SN_0 remains more or less constant. Though the gradient increases, the S_P decreases as defined in Equation 19.

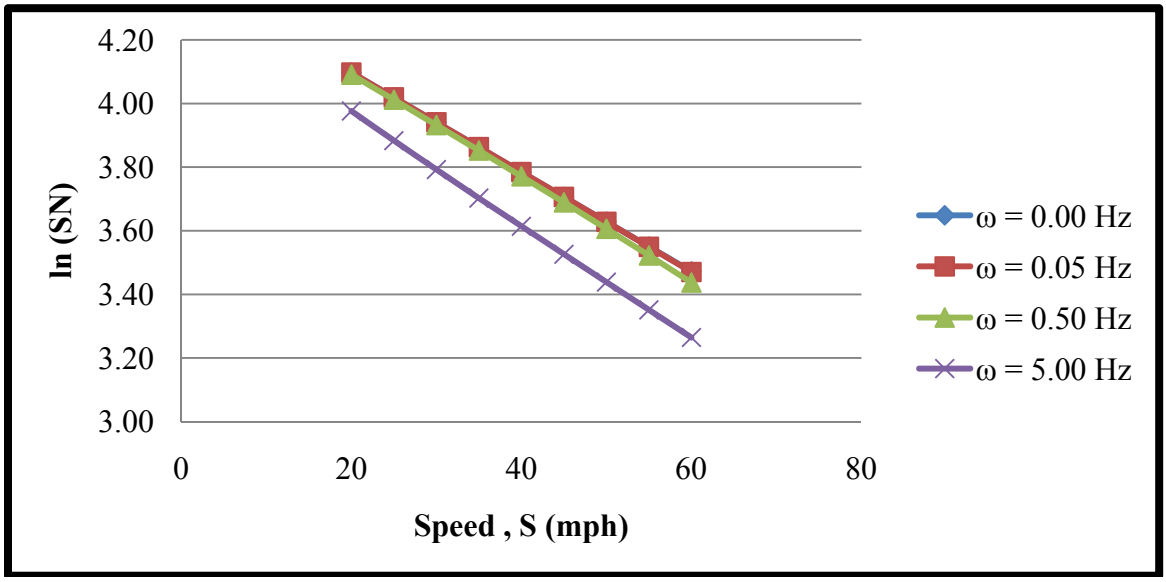

Figure 2-21: Frequency Variation Effects on the Friction-Speed Relationship of Pavement D

Table 2-10: Results of Frequency Variation Analysis on Pavements C and D

Pavement Characteristics	Frequency, ω (Hz)	Speed Gradient, S_P	SN_0
Pavement C	0.00	227.27	54.21
Pavement C	0.05	227.27	54.22
Pavement C	0.50	217.39	54.39
Pavement C	5.00	200.00	52.28
Pavement D	0.00	64.10	82.29
Pavement D	0.05	63.69	82.36
Pavement D	0.50	61.35	83.20
Pavement D	5.00	56.18	75.71

Similar to the previously performed frequency variation analysis, an amplitude variation analysis was conducted on Pavements C and D. Table 2-11 demonstrates the input values used in the program *LWT Prediction Model*. Figures 2-22 and 2-23 display the results of the inputs from Table 2-11.

Table 2-11: Inputs for Frequency Variation Analysis (ω = 0.05 Hz)

Pavement	Amplitude, A (m)			
C	0.00	0.05	0.50	5.00
D	0.00	0.05	0.50	5.00

The magnitudes of SN_0 and the changes of the slope of the friction-speed relationship (speed gradient) for Pavements C and D are shown in Table 2-12. As seen in Table 2.12, for a given pavement, as the amplitude increases, the gradient of the friction versus speed curve increases while SN_0 remains more or less constant. Though the gradient increases, the S_P decreases as defined in Equation 19.

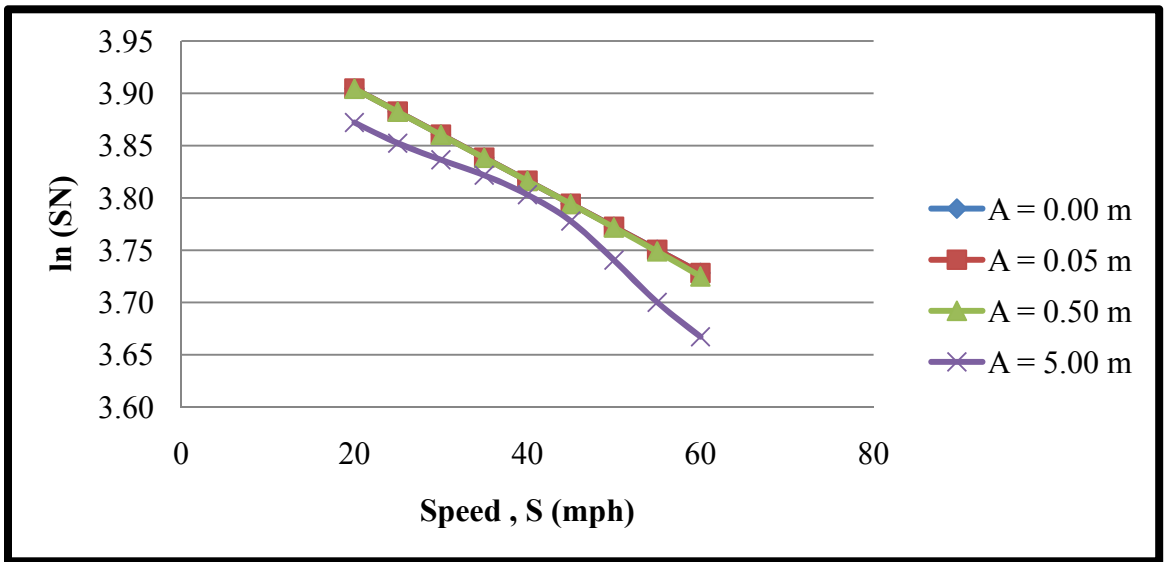

Figure 2-22: Amplitude Variation Effects on the Friction-Speed Relationship of Pavement C

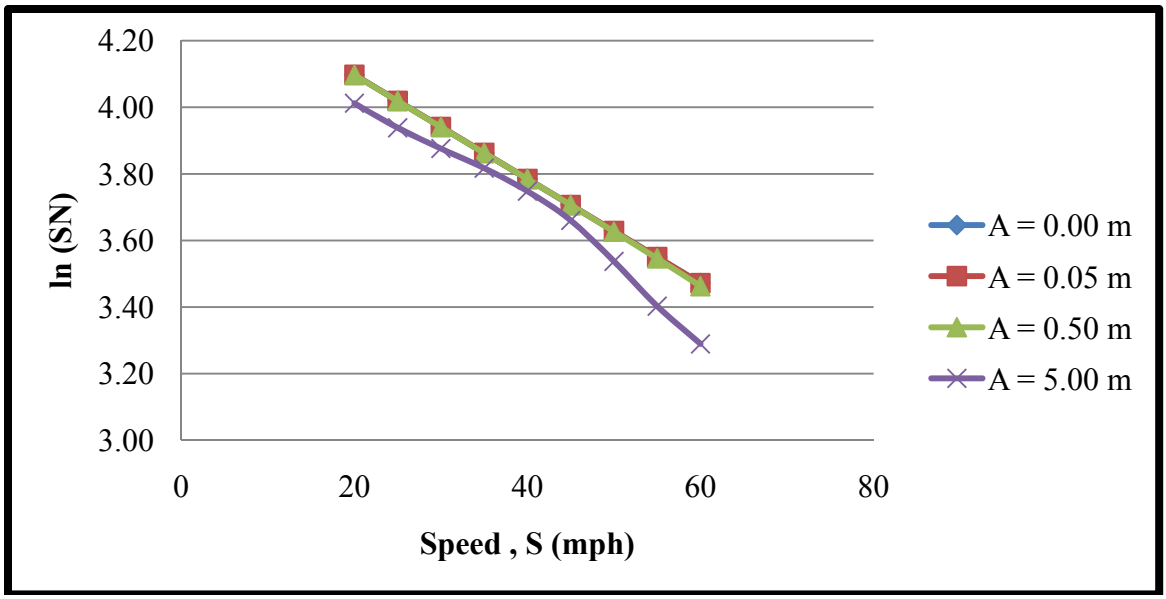

Figure 2-23: Amplitude Variation Effects on the Friction-Speed Relationship of Pavement D

Table 2-12: Results of Amplitude Variation Analysis on Pavements C and D

Pavement Characteristics	Amplitude, A (m)	Speed Gradient, S_P	SN_0
Pavement C	0.00	227.27	54.21
Pavement C	0.05	227.27	54.21
Pavement C	0.50	222.22	54.29
Pavement C	5.00	200.00	53.91
Pavement D	0.00	64.10	82.29
Pavement D	0.05	64.10	82.29
Pavement D	0.50	63.29	82.67
Pavement D	5.00	56.18	82.22

Due to the limited amount of data on the ***SN*** versus normal load relationship for different types of pavements, this analysis was designed to illustrate typical results that would be seen on most pavements.

2.8 Field Verification of the Effects of Pavement Roughness on the IFI

As shown in Section 2.7, pavement roughness can have a significant effect on the measured SN values and hence the computation of the IFI. Another aspect of the Fuentes [5] experimentation consisted of analyzing the effects of pavement roughness on measured skid values. Based on the analysis in Section 2.7, the variation in S_P can be significantly different depending on the frequency and amplitude variations along a given pavement. This difference was verified in the field using data from Fuentes' [5] original experiment, as well as friction tests conducted on an alternative Pavement I located in Brandon, Florida. The friction testing on Pavement I was conducted using the same protocol used by Fuentes to ensure that the results would not be skewed. In this regard, two sections were evaluated on Pavement I with one section found to be relatively rougher compared to the other, based on the significantly different profiles.

After evaluating the macrotexture using the CT Meter to ensure that macrotexture was identical on both of those sections, skid tests were performed on the two pavement sections with significantly different profiles. Reformulation of data from Fuentes' [5] experiment on Pavement B is shown in Figure 2-24, with Table 2-13 displaying the values of SN_0 and S_P. The values of SN_0 from these two sections are not significantly different, and it can be inferred from regression that the friction at zero speed is invariant for both pavement sections. On the other hand, Figure 2-25 shows the data from testing of Pavement I with Table 2-14 displaying the values of SN_0 and S_P.

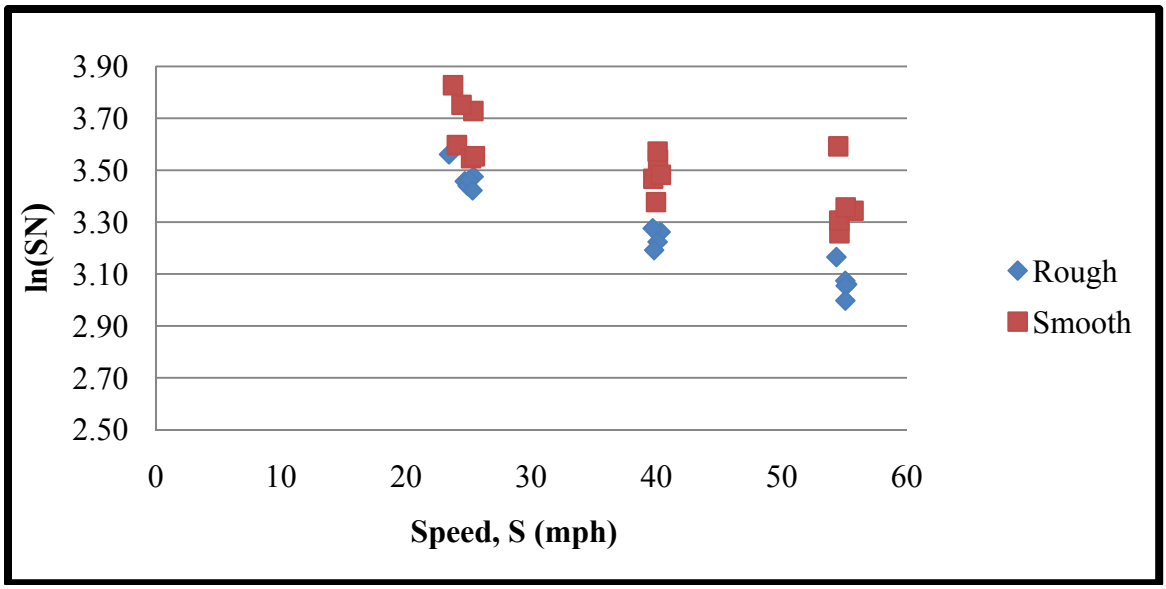

Figure 2-24: Effect of Pavement Roughness on IFI Parameters for Pavement B

Table 2-13: Results from Pavement Roughness Analysis on Pavement B

Section	Speed Gradient, S_P	SN_0
Smooth	100.00	49.74
Rough	74.63	44.46

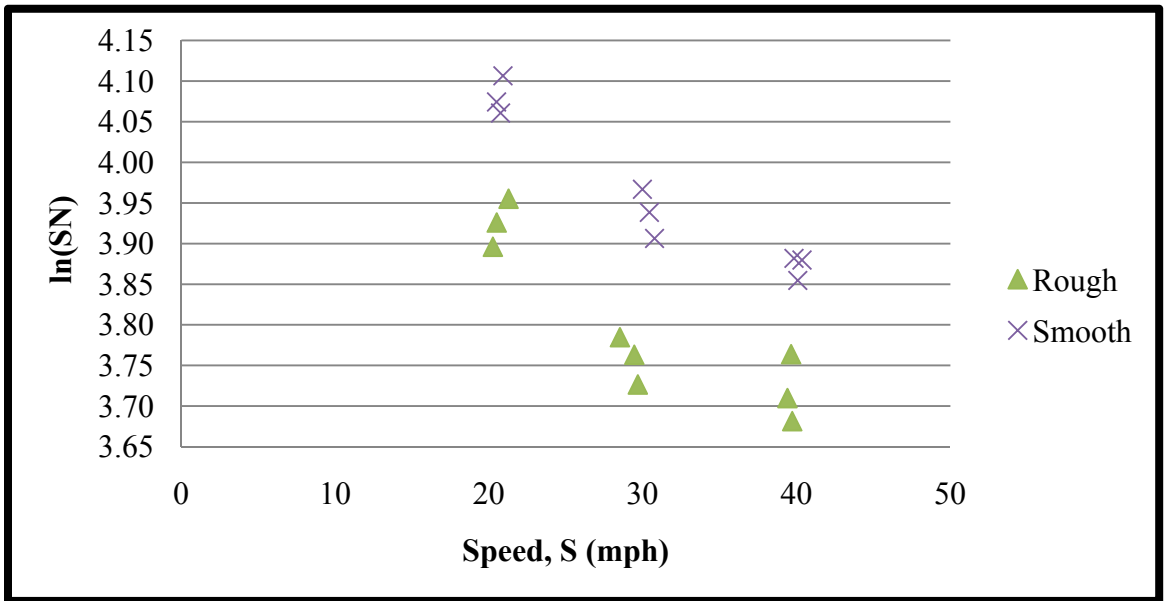

Figure 2-25: Effect of Pavement Roughness on IFI Parameters for Pavement I

Table 2-14: Results from Pavement Roughness Analysis on Pavement I

Section	Speed Gradient, S_P	SN_0
Smooth	92.59	73.05
Rough	93.46	61.52

The values of $\boldsymbol{SN_0}$ for both sections on Pavement B is more or less constant, while the SP decreases as the roughness increases. This follows the predictions made by the program *LWT Prediction Model.* However, the values of $\boldsymbol{SN_0}$ for both sections of Pavement I are significantly different, and it was concluded that regression data is needed from higher speeds to make an appropriate conclusion about their relationship. The $\boldsymbol{S_P}$ variation for the Pavement I sections also does not conform to previous findings in this work, and it was concluded that tests at higher speeds are needed to determine to true gradients of each section of pavement. Review of these two sets of data shows that the IFI parameters must be calculated from a larger range of speeds in order to be valid.

2.9 Modeling the Effects of the Normal Load versus Friction Load Relationship

The friction load predictions for the LWT were made in this work primarily based on the relationship between ***SN*** and normal load developed by Fuentes [5]. Therefore it is clear that the relationship of ***SN*** to normal load is critical to predicting the friction load response of the LWT from the program *LWT Prediction Model*. Hence, an investigation was conducted to explore in detail the effects of the above relationship on skid resistance measurements.

Equation 20 expresses $\boldsymbol{\Delta SN}$, which is maximum difference between ***SN*** observed during changes in the normal load of a given pavement and hence expressed by;

$$\Delta SN = SN_i - SN_r \quad (20)$$

Using data from Pavement C in the Fuentes [5] experiments, three other hypothetical pavements (Pavement E, F, and G) were created with the same SN_i but having different ΔSN values to model the effects of the friction-speed relationship measured with the LWT. Figure 2-26 displays the representative SN versus normal load relationships of the pavements used in the above analysis, while Figure 2-27 shows the variation of ΔSN versus speed of the hypothetical pavements matching that of Pavement C.

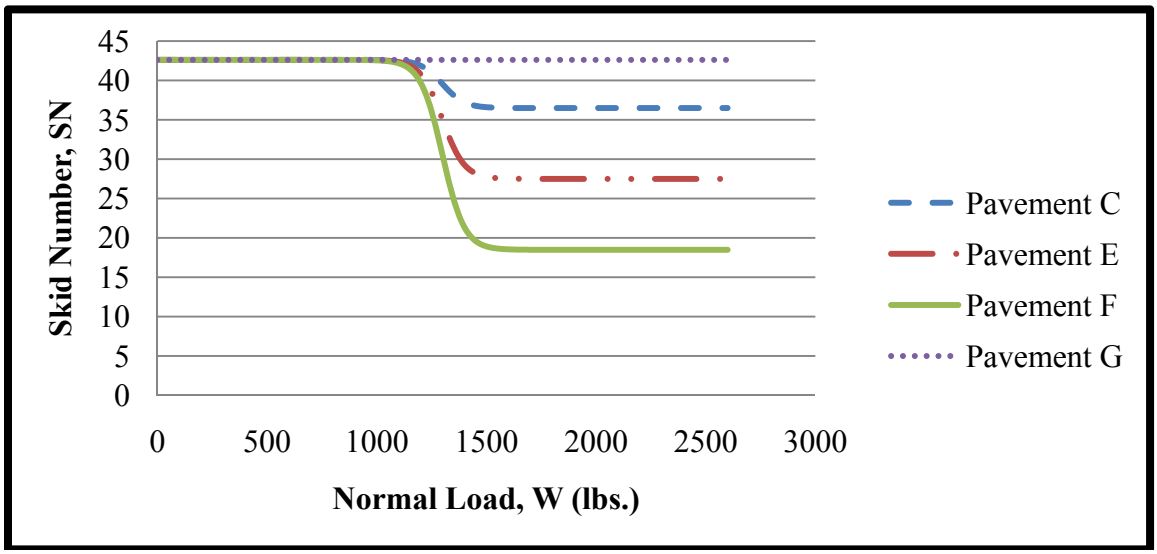

Figure 2-26: Relationship of SN vs. Normal Load for Pavements C, E, F, and G at 55 mph

Using the data in Figures 2-26 and 2-27 an analysis was performed with the program *LWT Prediction Model* to determine the effect of ΔSN of a given pavement on measured friction values. While the results are displayed in Figure 2-28, and the magnitudes of the changes are displayed in Table 2-15.

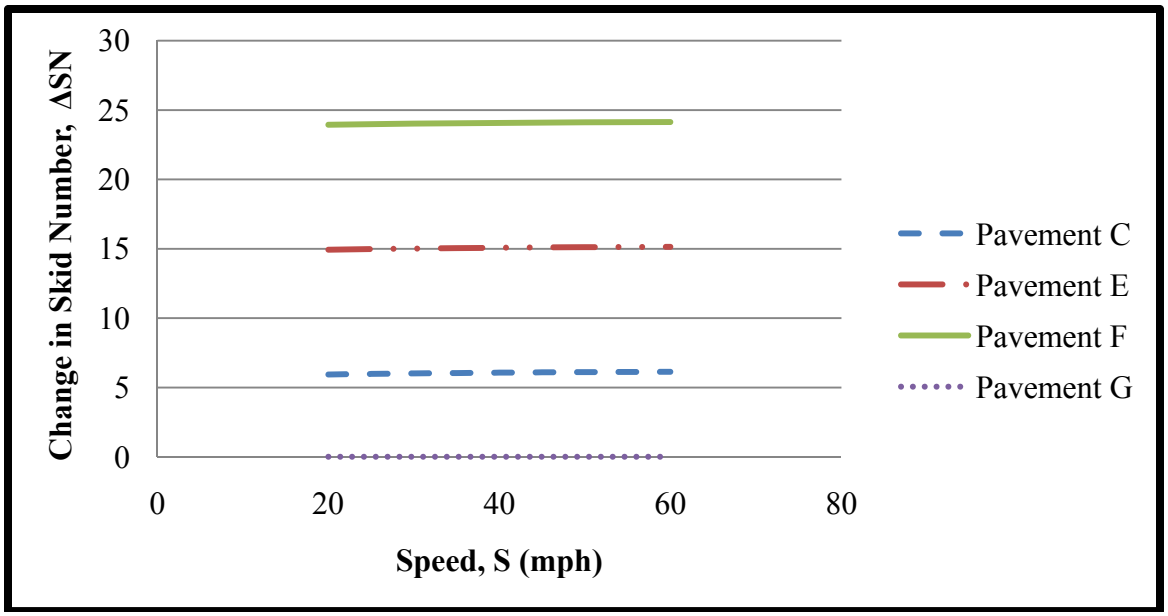

Figure 2-27: Variation in ***ΔSN*** versus Speed for Pavements C, E, F, and G

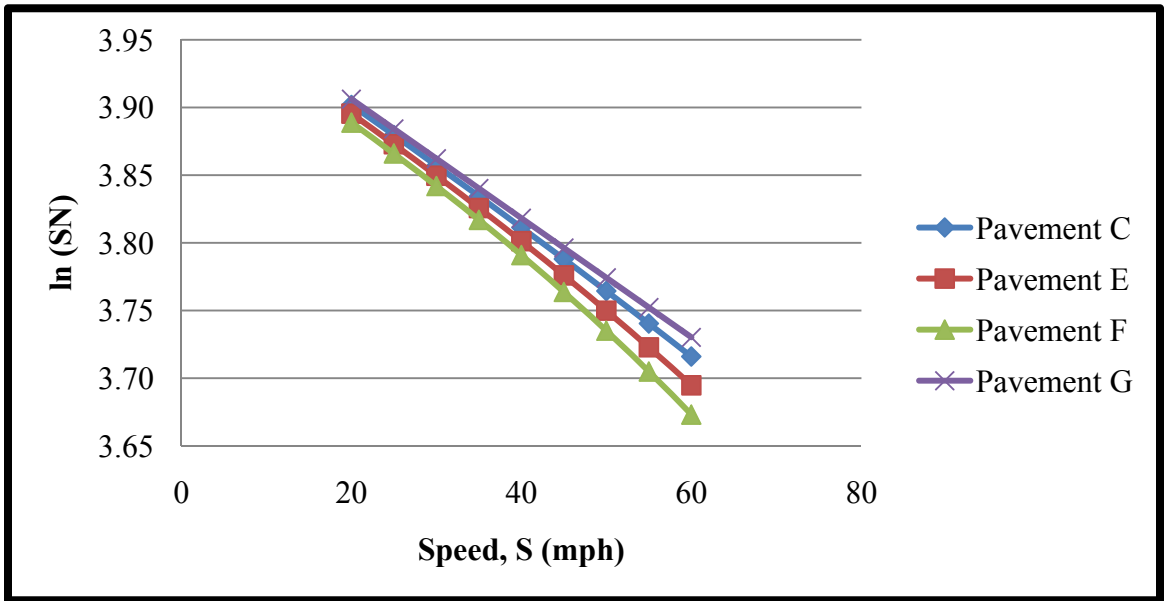

Figure 2-28: Effects of Variation in ***ΔSN*** for Pavements C, E, F, and G with Speed

Table 2-15: Results from ***ΔSN*** Variation Analysis on Pavements C, E, F, and G

Pavement	Speed Gradient, S_P	SN_0
Pavement C	217.39	54.39
Pavement E	200.00	54.54
Pavement F	185.19	54.71
Pavement G	227.27	54.28

The results in Table 2-15 confirm that the ***ΔSN*** of a given pavement can have a significant effect on the speed gradient, S_P, and hence the measured friction values. This effect is also illustrated in Figures 2-24 and 2-25 where the pavements are seen to have significant differences in particular the S_P values. In summary, it can be concluded that three factors will affect the computed IFI values of a rough pavement:

1. Frequency of roughness wave
2. Amplitude of roughness wave
3. ***SN*** dependence on the normal load (***ΔSN***)

2.10 Alternative Method for Determining Relationship Between SN and Normal Load

In lieu of the rigorous method by which Fuentes [5] determined the relationship of ***SN*** versus normal load for a given pavement, this study proposes a more practical method for the convenience of implementation. Data from Pavement B in Fuentes' [5] experiment was reformulated to reflect the relationship given by Schallamach in Equation 7. The average normal loads of each section were normalized using a static LWT weight of 1085 lbs. and then plotted against the corresponding ***SN*** of those tests. The basic form of Equation 7 used in this analysis is given in the following equation;

$$SN = c\left(\frac{W_{AVE}}{W_{STATIC}}\right)^{-a} \quad (21)$$

where ***c*** is the speed-dependent parameter, ***a*** is a parameter specific to the pavement type, W_{AVE} is the average normal load recorded during a more or less uniformly rough section, and W_{STATIC} is the static weight of the LWT. Figure 2-29 shows the plots of Equation 21 at speeds of 25, 40 and 55 mph.

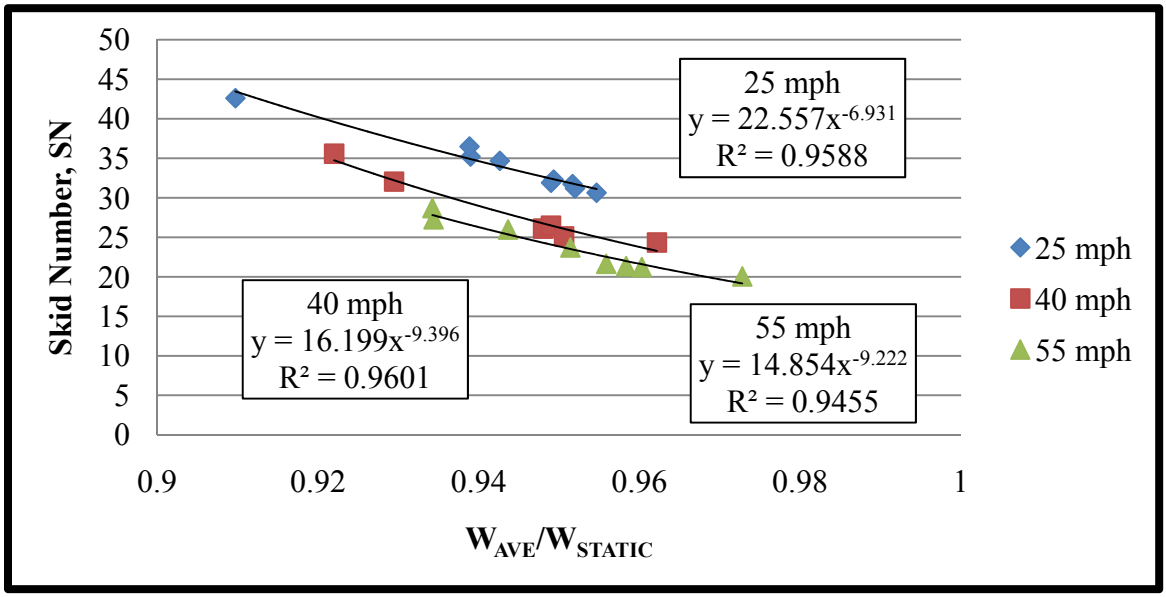

Figure 2-29: Relationship of ***SN*** vs. Normal Load for Pavement A at 25, 40, and 55 mph Using Schallamach's Equation

Based on Figure 2-29, the mathematical form prescribed in Equation 21 seems to provide a valid method for determining the relationship of ***SN*** versus normal load. The parameter ***a*** is nearly identical at 40 and 55 mph, showing that ***a*** can be assumed to be invariant for this pavement. The value of ***a*** at 25 mph is slightly different from those at 40 and 55 mph, but friction testing at low speeds has been found to be relatively unreliable and inconsistent due to the back-torque effect as outlined in Section 2.4. The values of ***c***

decrease as speed increases, which follows the basic tenants of the friction-speed relationship.

In order to develop these trends for other pavements, friction tests must be conducted at least on two relatively rough and smooth sections of a given pavement, and the resulting average normalized weights must be plotted against the average ***SN*** values as in the case of Figure 2-29. This procedure was followed on Pavement I from Section 2.8, and the results are given in Figure 2-30.

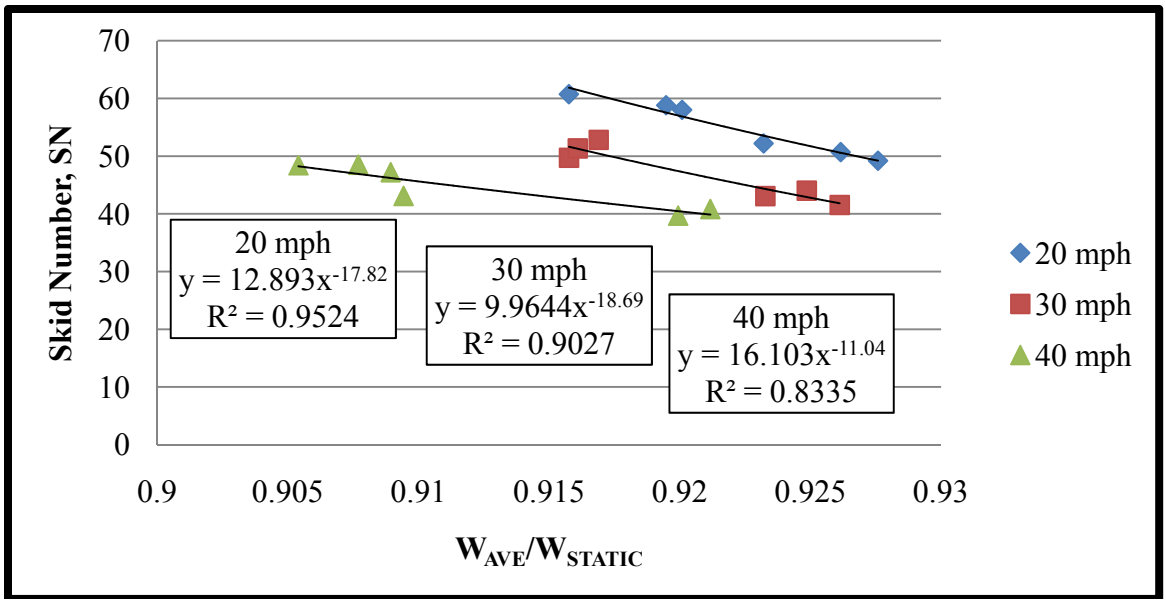

Figure 2-30: Relationship of ***SN*** vs. Normal Load for Pavement I at 20, 30, and 40 mph Using Schallamach's Equation

Review of Figure 2-30 shows that the pavement parameter ***a*** varies slightly across the speeds tested. Also, the speed-dependent parameter c is skewed at 40 mph. In addition, the relatively low R^2 at 40 mph indicates possible error in the data at that speed.

CHAPTER 3

CONCLUSIONS AND RECOMMENDATIONS

3.1 Current Research Proponents

Evaluation and maintenance of pavement friction in a highway network is a crucial aspect of transportation safety programs. Researchers have made significant efforts to evaluate and standardize pavement friction measured with numerous full-scale friction testers. In this work, an attempt has been made to understand the frictional response of the LWT for a given profile. A two degree of freedom vibration model was developed to simulate the LWT behavior and determine what effects pavement roughness has on the LWT measured friction and hence the IFI value of a given pavement profile.

3.2 Contribution 1 - Theoretical Prediction of LWT Friction Values

As outlined in Section 2.6, measured friction values can be predicted accurately using the program *LWT Prediction Model* developed in this study. The ability of the program *LWT Prediction Model* to predict friction on a given pavement is governed by the frictional dependency of that pavement on the normal load. This relationship was also shown to affect significantly the reported values of the IFI due to its effect on the speed gradient, S_P. Further modification of this method must be pursued by better evaluating the dependency of friction on the normal load.

3.3 Contribution 2 - Effects of Pavement Roughness on the IFI

As outlined in Section 2.7, pavement roughness can have significant effects on the computed IFI values of a pavement. As the roughness of a pavement increases, the friction-speed relationship is altered, thus changing the values of S_P and F_{60}. Using linear regression of the data, it was shown that various friction-speed plots merge on a single value of SN_0 (SN at zero speed). The author's LWT model predicts that generally the S_P of a pavement decreases as pavement roughness increases.

3.4 Contribution 3 - Effects of Frictional Dependency on Normal Load on the IFI

In lieu of the relatively complicated process in which the SN vs. W relationship was developed by Fuentes [5], a new method was proposed to facilitate the prediction of SN values from the developed program. Using the form prescribed by Schallamach and the method outlined in Section 2.10, practitioners can accurately develop an appropriate relationship between SN and normal load for a given pavement. Ideally, the parameters in Equation 21 can be standardized based on macrotexture values, and then input into the author's model to accurately predict pavement friction over any given profile. Pavements with large ΔSN values (maximum SN difference with respect to the normal load) were shown to be more sensitive to roughness and produce larger deviations in the IFI parameter. This effect can be minimized if pavements could be designed with materials that exhibit a minimal SN variation (ΔSN). For instance, a pavement with ΔSN of zero would exhibit no effects due to pavement roughness or elevated DLC.

LIST OF REFERENCES

[1] Leu, M.C. and J.J. Henry. “Prediction of Skid Resistance as a function of Speed from Pavement Texture,” Transportation Research Record 946, Transportation Research Board, National Council, Washington, D.C., 1983.

[2] Wambold, J. C., C. E. Antle, J. J. Henry, and Z. Rado. “International PIARC Experiment to Compare and Harmonize Texture and Skid Resistance Measurements”. Final Report submitted to the Permanent International Association of Road Congresses (PIARC), State College, PA, 1995.

[3] ASTM: “Standard Practice for Calculating International Friction Index of a Pavement Surface”, Standard No E1960-07, ASTM 2009

[4] ASTM: “Standard Test Method for Skid Resistance of Paved Surfaces Using a Full-Scale Tire”, Standard No E274-06, ASTM 2009

[5] Fuentes, L., M. Gunaratne, and D. Hess. “Evaluation of the Effect of Pavement Roughness on Skid-Resistance,” ASCE Journal of Transportation Engineering, Vol. 136 No. 7, Reston, Virginia, 2010.

[6] Schallamach, A. “The Load Dependence of Rubber Friction”, Proc. Phys. Soc., Section B, Volume 65, Issue 9, pp. 657-661 (1952).

[7] Das, B.M. “Fundamentals of Soil Dynamics”. New York: Elsevier Science Publishing Co., Inc., 1983. Print.

[8] Inman, D. J., “Vibration with Control”. New York: John Wiley and Sons, Ltd, 2006. Print.